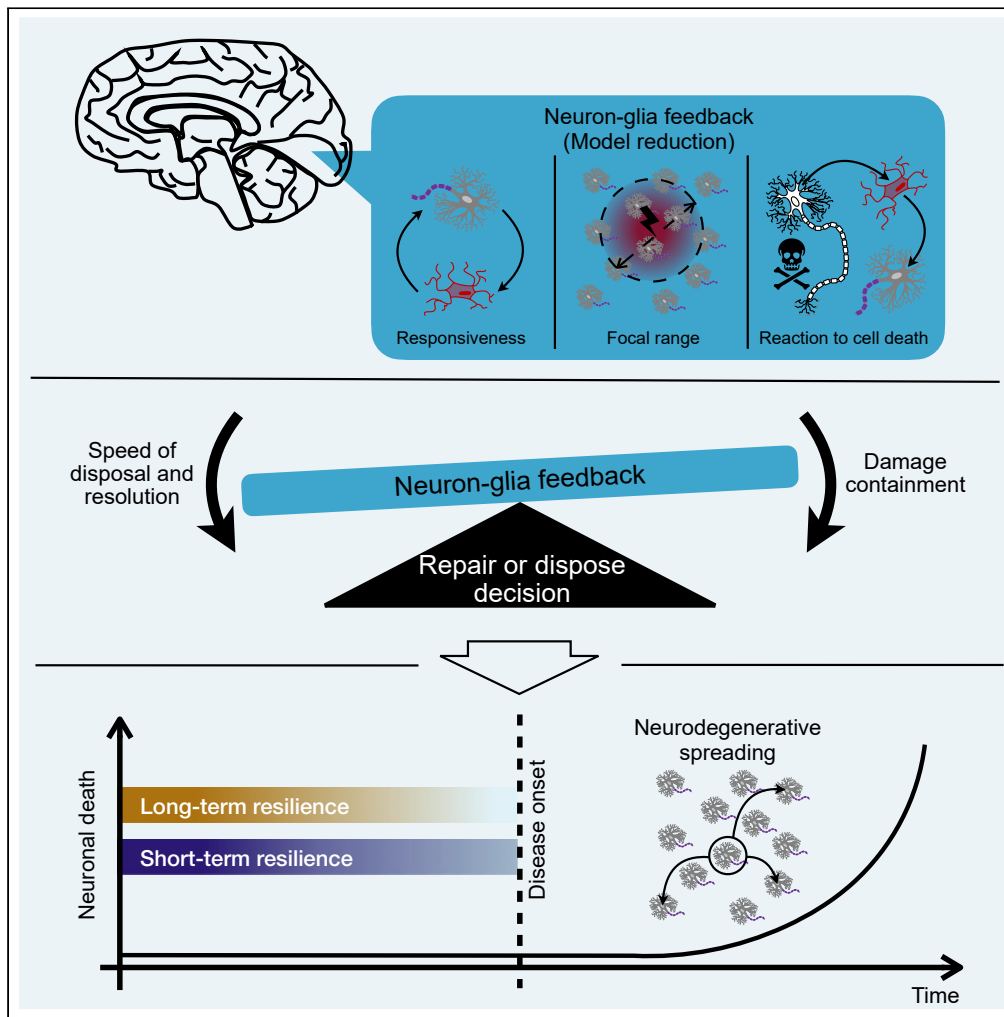


Article

How Repair-or-Dispose Decisions Under Stress Can Initiate Disease Progression



Andreas Nold,
Danylo Batulin,
Katharina Birkner,
Stefan Bittner,
Tatjana
Tchumatchenko

andreasnold@me.com (A.N.)
tat@tchumatchenko.de (T.T.)

HIGHLIGHTS

We present a computational model for disease onset of neurodegeneration

Healthy neuron-glia crosstalk balances seed removal and resolution of inflammation

Warning signs prior to onset are slowed reactivity and increased collateral damage

Analogous processes are found in Alzheimer disease and multiple sclerosis



Article

How Repair-or-Dispose Decisions Under Stress Can Initiate Disease Progression

Andreas Nold,^{1,5,*} Danylo Batulin,^{1,2} Katharina Birkner,³ Stefan Bittner,^{3,4} and Tatjana Tchumatchenko^{1,4,*}

SUMMARY

Glia, the helper cells of the brain, are essential in maintaining neural resilience across time and varying challenges: By reacting to changes in neuronal health glia carefully balance repair or disposal of injured neurons. Malfunction of these interactions is implicated in many neurodegenerative diseases. We present a reductionist model that mimics repair-or-dispose decisions to generate a hypothesis for the cause of disease onset. The model assumes four tissue states: healthy and challenged tissue, primed tissue at risk of acute damage propagation, and chronic neurodegeneration. We discuss analogies to progression stages observed in the most common neurodegenerative conditions and to experimental observations of cellular signaling pathways of glia-neuron crosstalk. The model suggests that the onset of neurodegeneration can result as a compromise between two conflicting goals: short-term resilience to stressors versus long-term prevention of tissue damage.

INTRODUCTION

Throughout our lifetime the brain faces the challenge of keeping neuronal networks functional under widely varying conditions. This requires repairing injured neurons or, if their damage is irreversible, disposing of them in order to maintain global tissue health. This decision is made largely by glia-neuron crosstalk in the brain (Brown and Neher, 2014; Aguzzi et al., 2013; Barres, 2008) and needs to be critically balanced because neurons are postmitotic cells, and stem-cell niches have only a limited potential for regeneration (Barres, 2008). One of the long-standing challenges in clinical neuroscience is to understand how the brain upholds its amazing resilience capacity, and how glia-neuron interactions contribute to it.

As a diverse set of cells, glial cells consist of astrocytes, microglia, and oligodendrocytes among others, each playing a vital role in protecting neurons from harm, supplying nutrients, and establishing an environment where neurons can thrive. For example, astrocytes respond to threats such as external trauma or inflammation by transitioning to a “reactive” proinflammatory phenotype (Khakh and Sofroniew, 2015). Microglia constantly surveil their local microenvironment and clear the tissue of pathogens and phagocyte synapses or dead cell material (Nimmerjahn et al., 2005). Oligodendrocytes help maintain axonal health and defend against the threatening factors to axonal integrity by eliciting an increase of precursor cell differentiation and increasing remyelination (Nave and Trapp, 2008).

Importantly, neurons communicate directly with glia to signal their health state and either suppress or increase glial activity (Biber et al., 2007). The endogenous glia-neuron feedback loop normally responds to perturbations in a way that a lesion is contained and neuronal network function is maintained. Malfunction of this feedback can be triggered by a variety of causes ranging from trauma (Lozano et al., 2015), inflammation, stroke (Broughton et al., 2009), and break-down of the blood brain barrier (Pinheiro et al., 2016) to aging (Grabert et al., 2016), ultimately leading to neurodegeneration and functional deficits. Upon intrinsic and external stressors, the severity of the neuronal loss and how quickly it spreads depends significantly on the functionality of the glia-neuron feedback loop, suggesting a critical role for this communication in maintaining brain resilience (Henstridge et al., 2019; Hickman et al., 2018; Heneka et al., 2018).

One crucial aspect for the functionality of glia-neuron feedback is the balance between repair and dispose-inducing tissue reactions. In healthy tissue, both modes are tightly controlled by checkpoint mechanisms and a web of complex cellular interactions (Deczkowska et al., 2018). We consider the net effect of this complex array of interactions: the repair or disposal of damaged neurons. We put forward a dynamical model

¹Theory of Neural Dynamics, Max Planck Institute for Brain Research, 60438 Frankfurt am Main, Germany

²Frankfurt Institute for Advanced Studies (FIAS), 60438 Frankfurt am Main, Germany

³Department of Neurology, Focus Program Translational Neuroscience (FTN), University Medical Center of the Johannes Gutenberg University Mainz, 55131 Mainz, Germany

⁴These authors contributed equally

⁵Lead Contact

*Correspondence: andreasnold@me.com (A.N.), tat@tchumatchenko.de (T.T.) <https://doi.org/10.1016/j.isci.2020.101701>



that mimics this process and study the implications that a dysregulation of the repair-or-dispose decision process can have for disease progression. By following a reductionist approach, we aim to produce a plausible hypothesis for the basic tissue behavior at the onset of disease progression. But, how viable is it to use a reductionist mathematical model to understand a process of enormous complexity such as the glia-neuron crosstalk in the context of highly complex and diverse neurodegenerative diseases?

In the last couple of decades, several modeling approaches have been put forward to better understand processes underlying neurodegeneration and neural tissue resilience (Kolodkin et al., 2012; Anderson and Vadigepalli, 2016; Lloret-Villas et al., 2017). The modeling approaches vary widely and address aspects ranging from nervous system energy metabolism (Cloutier et al., 2009; Lewis et al., 2010), protein degradation (Cloutier and Wellstead, 2012; Ouzounoglou et al., 2014), and blood-brain barrier transport (Garg and Verma, 2006; Martins et al., 2012) to tauopathy (Proctor and Gray, 2010; Yuraszeck et al., 2010). For example, studies that focus on the role of a particular signaling pathway typically aim to capture a specific biochemical process as accurately as possible (Fussenegger et al., 2000; Proctor and Gray, 2010; Tang et al., 2010; Proctor and Lorimer, 2011). Typically, the mathematical model consists of a set of biochemical reactions, e.g. describing the interplay between protein synthesis, folding, refolding, degradation, and aggregation (Proctor and Lorimer, 2011). However, the detailed model design requires strong assumptions about the conditions in which it is valid and often hinges on extensive use of *in vitro* data for parameter estimation and model verification. This limits the explanatory and predictive power for the overall disease progression. Computational models that target processes by multiple agents and/or on several timescales require higher levels of abstraction.

One such approach is followed by data-driven models. Such models can, for example, predict the mortality risk for traumatic brain injury patients based on clinical variables such as age, gender, and discretely monitored inflammatory biomarkers (Constantine et al., 2016; Abboud et al., 2016). However, the data-driven design principle often does not allow to infer a mechanistic understanding of underlying disease processes. To achieve this, abstract models are used, which capture a selection of specific mechanisms. These abstract dynamical models address a broader aspect of disease progression at the expense of detail by model reduction. In contrast to data-driven models, which infer quantitative predictions based on past observations, the primary goal of abstract models is to generate hypotheses and drive conceptual insights into disease processes. For example, a neuronal mass model of partial epileptic seizures (Jirsa et al., 2014) models transitions between healthy nervous system activity and seizure-like events using only five state variables and is used in basic research on epilepsy (Chizhov et al., 2018; Zhang and Xiao, 2018) and in clinical studies (El Houssaini et al., 2019). In the field of neurological diseases, diffusion models (Weickenmeier et al., 2018) and epidemic spread models for misfolded protein dynamics (Itria-Medina et al., 2014; Vogel et al., 2020) have linked the spread of toxic proteins in 3D brain structures with spatiotemporal patterns of pathology development. The main challenge for the development of such dynamical models is to determine an abstraction level which follows existing evidence and shows a distinct enough behavior that can be used to generate a hypothesis. We believe that the understanding of glia-neuron crosstalk and neurodegenerative disease processes has advanced enough to put forward a model for the interaction between fast repair-or-dispose decisions in glia-neuron crosstalk and slow disease progression.

We adopt a reductionist computational model to generate a hypothesis about how such a self-cleaning mechanism might work and fail (see Figure S1). The model includes two coarse grained state variables of an assembly of cells. External stressors can induce local cell damage. If untreated, these cells then damage connected cells, therefore compromising functionality and stability of the cell assembly. The system therefore includes a self-cleaning mechanism by which damaged cells are disposed of. Model computations based on these core assumptions reveal four distinct states for the assembly: healthy, challenged, primed, and chronic. Importantly, they show that with rising baseline damage, the self-cleaning mechanism needs to satisfy two conflicting goals: it needs to recognize and remove damaged cells and at the same time avoid collateral damage. The result of this tug-of-war between long- and short-term resilience determines how long the cell assembly can be maintained within the context of the model. The manuscript is structured as follows: we set up the model and present its functional modes in the Results section. We then discuss analogies to cellular processes and to experimental and clinical findings for neurodegenerative disease courses. Finally, we suggest a mechanistic explanation for the progression of Alzheimer's disease (AD) and multiple sclerosis and discuss limitations of the approach.

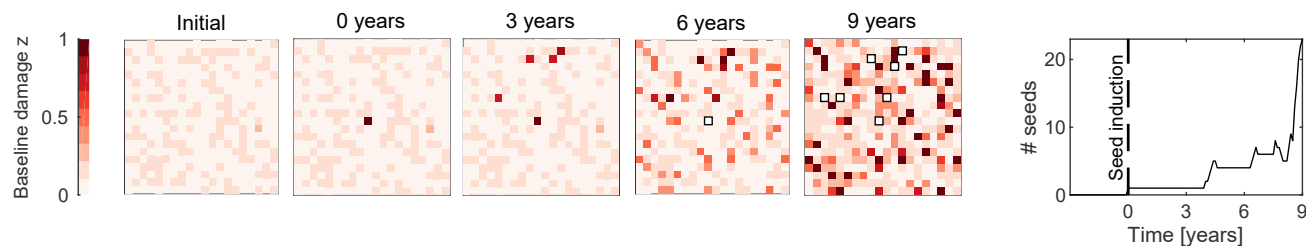


Figure 1. Exponential Spread of Baseline Damage z After Seed Induction

At time $t = 0$, a seed is induced in an otherwise healthy tissue of 20×20 cells with mean baseline damage $z = 0.05 \pm 0.02$. The damage spreads from the seed with timescale $\tau_\infty = 10$ years (see Equation 1). Each cell receives damage from $M = 10$ other cells. Here, cells become seeds themselves if $z > 0.5$, and they die if $z = 1$ (white squares). Right panel: damage progression is characterized by a phase of slow subthreshold spread, followed by an exponential increase in the number of seeds. Note that the spread scales linearly with τ_∞ in time and is therefore qualitatively independent of the choice of τ_∞ .

RESULTS

Model

Similar to the spread of a virus from human to human in a pandemic, there are diseases in which damage propagates from cell to cell. For instance, in several neurodegenerative diseases, neurons can induce damage-inducing processes via synapses (see e.g. (Vogel et al., 2020; Uemura et al., 2020) and Discussion for further disease-specific processes). Such cells, which spread damage to connected cells, will be referred to as “seeds.” If not contained, then widespread tissue damage can initiate from a single seed. First, this seed increases damage in connected cells. Then, once these connected cells exceed a damage threshold, they become seeds themselves and also start propagating damage. Because every cell spreads damage to many other cells, this process accelerates exponentially. We are interested in the following scenario: first, we consider cases where damage spread from one cell to another cell is slow, in the range of weeks to years, but tissue maintenance is fast, in the timescale of hours to days. Second, we are interested in capturing the point of “ignition,” when the first seed successfully transmits damage, as accurately as possible by resolving the state of individual cells.

To formalize the spread in this scenario, each cell (with index n) is attributed one variable $z_n > 0$. This variable represents the “baseline damage” of the cell. We define the following three states based on z : if $z < z_{\text{cliff}}$, the cell does not spread damage. If $z_{\text{cliff}} < z < 1$, it becomes a seed and spreads damage to connected cells. Once $z = 1$, the cell dies. The lower z_{cliff} is, the higher is the tissue susceptibility for slow damage spread. Here, for simplicity we consider the intermediate case $z_{\text{cliff}} = 0.5$. The following equation formalizes the core process of such a spreading process:

$$\frac{dz_n}{dt} = \frac{1}{\tau_\infty} \sum_{m \in \mathcal{C}_n} [z_m - z_{\text{cliff}}]_+ \quad \forall n \in \mathcal{S}_{\text{alive}}(t), \quad (\text{Equation 1})$$

where τ_∞ is the duration of cell-to-cell transmission and $[z]_+ = z$ for $z > 0$ and zero otherwise. Each cell “receives” damage from M other cells. These potential damage transmitters are randomly selected for each cell and are defined by the set \mathcal{C}_n . Once a cell dies, it is excluded from \mathcal{C}_n and can no longer transmit damage. The process of damage spread is initiated by externally driven irreversible “seeding events.” For example, this could be an abnormal tau accumulation in AD (see Discussion for details). We assume that these seeding events are rare and sparse but that they will happen to some cells in the tissue. If left unchecked, they initiate devastating, exponentially increasing damage. Figure 1 shows the damage spread, starting from a single external seeding event. First, the seed induces damage to its connected cells, which then in turn spread damage. This cascade leads first to an exponential increase in the number of seeds and then an exponential increase of cell deaths. How can this undesirable result be avoided?

One effective way to avoid this spread is the quick removal of individual seed cells. The model therefore implements two fast mechanisms to maintain long-term tissue health: targeted removal of individual seed cells, and quick repair of subthreshold stress in cells (see e.g. (Brown and Neher, 2014; Biber et al., 2007) and Discussion for further cellular analogies). We then ask the question how and under which circumstances such a removal process can fail. The results can provide insights into what might be happening before a disease outbreak. For this, a useful seed removal model must only contain a very limited number of assumptions and parameters. The model proposed here (see Figure 2) is built on the following pillars: (1)

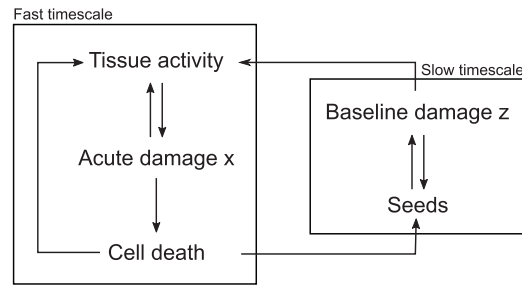


Figure 2. Model Setup

The model consists of slow and fast dynamics. Seed-driven damage spread is modeled by an increase in baseline damage at slow timescales (see Equation 1). Repair-or-dispose decisions are modeled at fast timescales (see Equation 2) as an interplay between acute damage and baseline damage. Once acute damage crosses a threshold, cell death is induced, which sets off a protective effect on neighboring cells. For analogous biological processes, see also Figure S1.

first, we assume seed removal is fast and happens within hours (timescale $\tau = 4$ hours) such that $\tau \ll \tau_\infty$. A second state variable is introduced to capture this quickly evolving acute damage x_n for each cell. In contrast to the baseline damage, which represents irreversible damage to a cell, acute damage is temporary. For example, it represents short-term damage to an axonal myelin sheaths. (2) Second, the removal-process itself stems from a nonlinear feedback loop of interactions within the tissue. For example, glia react to neuronal damage by activating a spectrum of states, which include anti- and pro-inflammatory phenotypes (Biber et al., 2007; Ransohoff, 2016). We therefore model the removal process as the result of a tug-of-war between damage-repairing and damage inducing tissue forces. Here, repairing forces are linear and pull the acute damage x toward the baseline damage z . Therefore, these forces act homeostatically in the short term by pushing the acute cellular state back to its baseline state. The damage-inducing forces are nonlinear and increase quadratically with acute damage and scale with the responsiveness parameter G . Here, we choose a quadratic term for simplicity to capture the increasing sensitivity, but other nonlinear terms are also possible. As a consequence of this tug-of-war, once a threshold of damage is passed, damage-inducing effects take over and drive the cell to cell death at $x = 1$ (see Figure 3). This is a bistable state: either the cells state is stably pulled to its baseline damage or it is driven to cell death. The transition point between these two states is determined by the parameter G . If G is too small, then damage-inducing nonlinear effects are not strong enough, and the system fails to drive a cell with high baseline damage to cell death (see Figure 3A). But if G is large enough, then nonlinear damage-inducing effects will be larger than homeostatic effects and the cell is driven to cell death. Taken together, such a removal mechanism with adequate choice of G quickly removes seeds from the tissue and stops the slow spread of damage in its tracks (see Figure 3).

The seed removal mechanism is formalized by (see also Figure 2)

$$\tau \frac{dx_n}{dt} = -r_n + d_n \quad \forall n \in \mathcal{S}_{\text{alive}}(t), \quad (\text{Equation 2})$$

where $\mathcal{S}_{\text{alive}}(t)$ is the set of alive cells at time t : $\mathcal{S}_{\text{alive}}(t) = \{n : x_n(t') < 1, \forall t' \leq t\}$. The first term $r_n = x_n - z_n$ represents (short-term) homeostatic forces that peg the acute to the baseline state. The second term d_n represents damage-inducing forces acting on cell n . To allow for visual inspection and to keep the model simple, we consider n cells as discrete units organized on a periodic equidistant lattice with grid spacing unity. Computations are performed on one- and two-dimensional lattices.

The tissue is an assembly of cells that do not act independently of each other. Cell-signaling mechanisms and cell migration (Stence et al., 2001; Tønnesen et al., 2018) mean that neighboring cells are impacted by the seed removal mechanism and by cell death (Savill and Fadok, 2000) at short timescales. This connectivity is different to the slow spread of baseline damage via C_n on long timescales τ_∞ . d_n samples the short-term damage-inducing and post-cell death effects from the neighborhood of the cell:

$$d_n = \sum_m s(|r_n - r_m|) g_m \quad (\text{Equation 3})$$

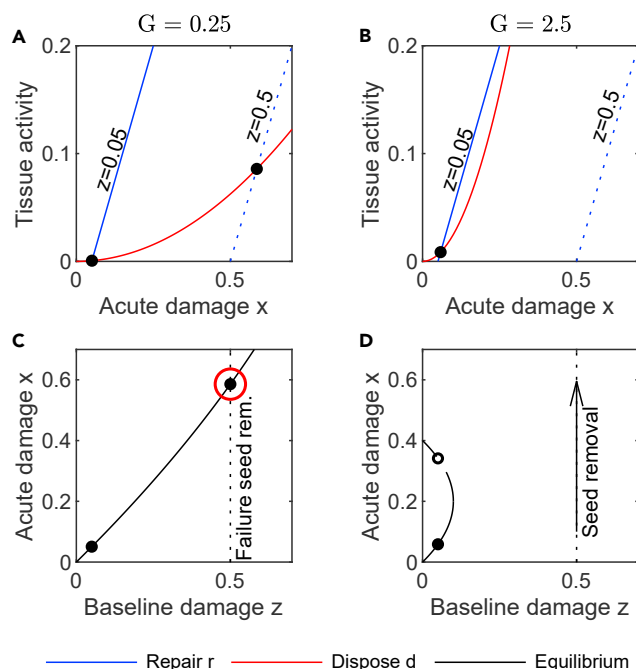


Figure 3. Repair-or-Dispose Decision

(A and B) Effects inducing repair ($r = x - z$, blue lines), and effects inducing disposal ($d = Gx^2$, red lines) for a system of a single cell, for scenarios with weak and strong responsiveness G (left and right columns) and low and high baseline damage z (solid and dashed blue lines). Black bullets show equilibrium states. (C and D) Equilibrium states as a function of baseline damage z . The system with low responsiveness G maintains the seed ($z = 0.5$) at elevated levels of acute damage. The system with high responsiveness G does not exhibit an equilibrium state for elevated baseline damage levels and drives these cells to cell death (“seed removal”) (see also Sec. S2 of [Transparent Methods](#)). See also [Figure S2](#).

where $r_{n,m}$ are positions of cells n and m , g_m are effects induced by cell m , and $s(r) \sim c^r$ describes that damage-inducing effects decrease by factor c in between cells (cells are organized on a lattice with spacing unity). We use this focal range $c \in [0, 1]$ as a measure for the spatial coupling. In the ideal case, cell signaling at short timescales implements a repair-or-dispose decision, which is perfectly tailored for each individual cell ($c \rightarrow 0$). If the tissue response is less precise, then $c > 0$ and the tissue response is “out of focus.”

The damage-inducing effect from neighboring cells can be attenuated. If a cell dies, then it typically has a protective effect on its neighbors (see [Discussion](#) for details). Here, we assume that this effect decays exponentially with time after cell death at time t_n^{death} with constant $\tau_{\text{death}} = 24$ hours and that it scales with D :

$$g_n = \begin{cases} Gx_n^2 & \text{if } n \in \mathcal{S}_{\text{alive}}(t) \\ D e^{-\frac{t-t_n^{\text{death}}}{\tau_{\text{death}}}} & \text{else} \end{cases} \quad (\text{Equation 4})$$

For details on the model see [Methods](#). [Figure 4](#) shows a typical seed removal process. After seed induction, damage-inducing tissue activity causes acute damage to both the seed and its surrounding tissue. This response of neighboring cells slows down the response similar to a form of inertia. Once a threshold is passed, acute damage accumulation accelerates, and the seed is driven to cell death. At this point, protective mechanisms are activated, and the surrounding tissue is “cooled down.”

Tissue States

Seed removal prevents long-term damage propagation as in [Figure 1](#) and is therefore crucial to maintaining long-term tissue health. A systematic study of seed removal in a cell assembly revealed that there exist four states: healthy tissue, challenged tissue, primed tissue prone to acute lesion spread, and chronically inflamed tissue (see [Table 1](#)). Each state is characterized by a signature of the four model parameters: baseline damage z , tissue responsiveness G , focal range c , and reaction to cell death D . It is the combination of



Figure 4. Seed Induction and Disposal

After seed induction at $t = 0$ hours at the center of a healthy tissue (baseline damage $z = 0.05 \pm 0.02$), the tissue increases disposal-inducing effects, due to its high responsiveness $G = 3$. Elevated levels of focal range $c = 0.4$ mean that surrounding tissue is affected too. The seed is subsequently driven to cell death ($x = 1$ at $t = 28$ hours), after which protective effects for the surrounding tissue are activated ($D = -1$, see Equation 4), and the remaining tissue returns to its homeostatic set point.

all four parameters that determines whether seed removal is successful or not. Consider first a healthy tissue, with low baseline damage.

In healthy tissue, the self-cleaning mechanism is intact and seeds are swiftly detected and removed (see Figure 4). Ideally, this state is characterized by low baseline damage z , high responsiveness G , a narrow focal range (low c), and a protective tissue reaction to cell death (low D). Short- and long-term resilience are maintained. In this state, the tissue detects single seeds and removes them with minimal effect on surrounding tissue. It therefore prevents the long-term spread of baseline damage. Also, its high responsiveness G means that seeds are removed quickly. This process can, however, also be inhibited.

An inhibited or slowed-down seed removal process is the hallmark of the challenged state. Challenged tissue exhibits increased values of baseline damage z and focal range c and requires a downregulation of tissue responsiveness G in order to maintain short-term stability. Notably, seed removal is still functional in this state. It is, however, slowed down and perturbations of the tissue are resolved at a slower pace (see Figure 5B). In particular, an increase of the focal range c has dramatic effects for seed removal. At first, removal is slower and puts more stress on the surrounding tissue (see Figure 5). The challenged phase is crucial for disease progression. Once the reserve of this phase is exhausted and seed removal fails, slow damage propagation takes over and the tissue transitions to the chronic phase.

The chronic phase is characterized by a widening of focal range c and loss of responsiveness G . This means that individual cells are maintained in the tissue, even though they have very high baseline damage levels (see Figures 5C, Sec. S3 and S2). This failure of seed removal leads to a breakdown of long-term resilience. In this state, tissue activity Gx^2 is high due to high levels of baseline damage z and high levels of acute damage x . This reflects a self-cleaning mechanism, which is constantly on high alert, but is ineffective. There is a positive side effect of this state: the downregulated responsiveness protects the tissue against unwanted short-term amplification of perturbations.

Such unwanted amplifications of perturbations are characteristic for the primed tissue state. In this state, the tissue appears to be healthy, but in the event of a sufficiently strong perturbation, a dysregulated self-cleaning mechanism exacerbates the effect of the perturbation, leading to a quickly spreading lesion

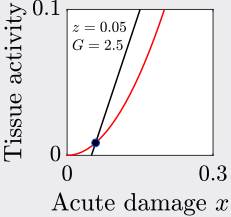
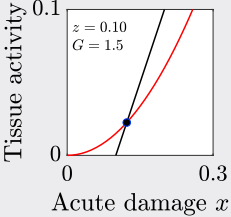
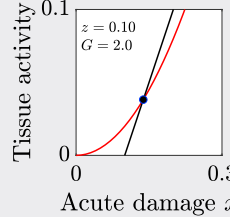
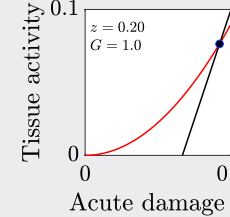
	(i) Healthy	(ii) Challenged	(iii) Primed	(iv) Chronic
Parameters				
Baseline damage z	Low	Elevated	Elevated	High
Responsiveness G	High	Elevated	Elevated	Low
Focal range c	Low	Elevated	High	High
Reac. to cell death D	Low	Low	High	Any
Behavior	Figure 4	Figure 5	Figure 6	Figures 1 and 5
Seed-removal	✓	slowed	slowed	✗
Contains perturbation	✓	slowed	✗	✓
Activity (Gx^2)	Focused, functional	Elevated	Damage-amplifying	High, dysfunctional
Clinical equivalent	Tightly regulated tissue surveillance; maintenance of short- and long-term resilience	Damage accumulation, lowered microglial motility; subclinical disease activity; driven by the periphery (e.g. RRMS)	Upregulated phagocytosis; primed microglia; immune training; acute lesion propagation	Dysregulated innate immune response; chronic neuronal stress; neurodegeneration; chronic inflammation (e.g. SPMS)

Table 1. Four Characteristic States of Tissue Resilience

(i) In the healthy state, z , c , and D are low, and high responsiveness G enables seed removal, therefore maintaining long-term resilience; (ii) under challenging conditions, i.e. increased baseline damage z and focal range c , the system becomes less stable, and seed removal gradually becomes less functional with decreasing responsiveness G ; (iii) if responsiveness G does not decrease, the system moves closer to a critical transition, and an acute attack can induce a quickly spreading lesion; (iv) in a highly damaged system, responsiveness is downregulated to ensure short-term stability. Nevertheless, high damage induces high levels of dysfunctional tissue activity. Insets show levels of damage-inducing (red lines, Gx^2) and damage-repairing (black lines, $x - z$) tissue activity as a function of acute damage x . The steady state is shown by a black dot at the intersection of both lines.

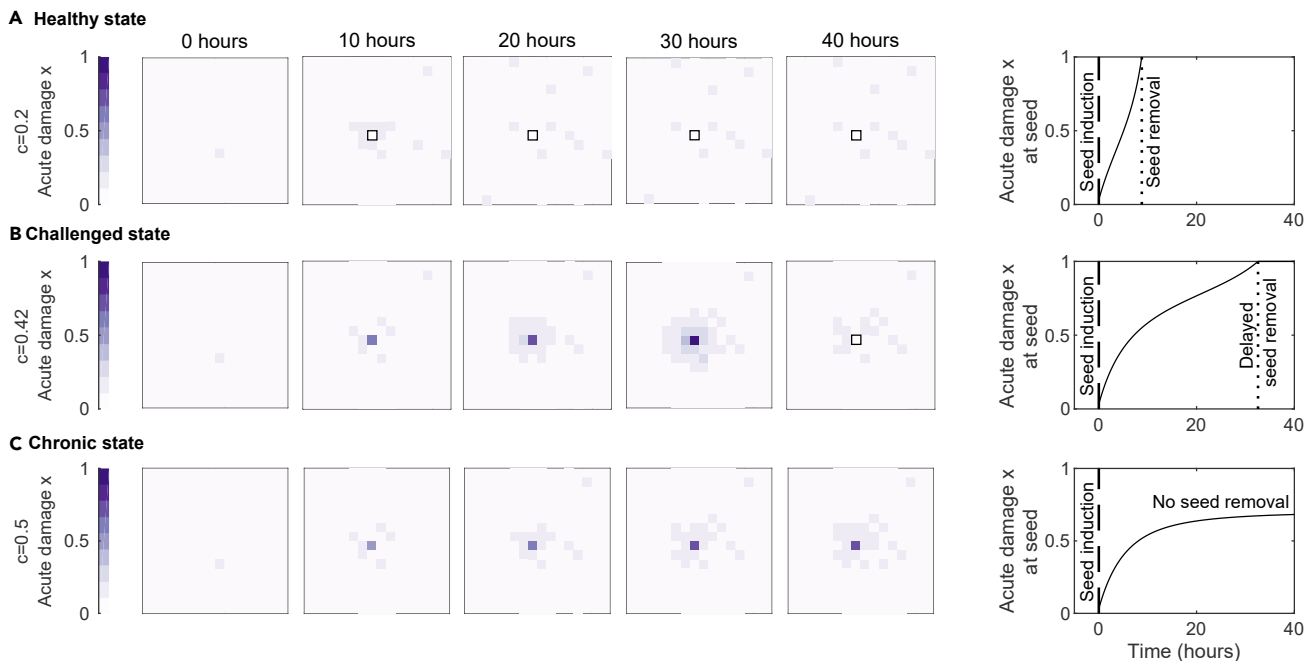


Figure 5. Increase of Focal Range c Induces Transition from Healthy to Challenged to Chronic State

Seed induction in a healthy tissue as in Figure 4, but with low ($c = 0.2$, (A)), increased ($c = 0.42$, (B)), and large ($c = 0.5$, (C)) focal range. Low focal range speeds up seed disposal. Increased focal range leads to delays in seed removal, and surrounding tissue is affected during seed removal. Further increase leads to failure of seed removal and persistent stress on the surrounding tissue.

(see Figure 6). The primed state can be aggravated and triggered more easily if reaction to cell death does not protect surrounding cells, therefore allowing for a fast domino-like lesion propagation (see Figures S3 and S4). In the event of a large shift in conditions, the whole system may become unstable, leading to spontaneous cell death across the tissue.

We conclude that whether seed removal is functional or not depends on the interplay between all parameters. So, which possibilities exist for the tissue to adapt to increasing baseline damage levels, e.g. in age and disease?

Tissue Adaptation

We consider two stress scenarios for different distributions of baseline damage $z < z_{\text{cliff}}$, i.e. before baseline damage spreads (see Equation 1). For this, we study Equation 2, 3, and 4 and set z as a parameter: in the first scenario, we homogeneously increase baseline damage z throughout the tissue. In the second scenario, we then consider a locally constrained increase in baseline damage (see Figure 7). We consider two measures for the tissue reaction: the time between seed induction and seed removal (see Figure 4) and the typical time the tissue takes to repair a small perturbation (see Methods for details). Both measures capture opposing effects: seed removal requires a strong local damage-inducing effect to drive the seed to cell death, but the repair time hinges on repair effects being stronger than damage-inducing effects. The tug-of-war between both defines the window of allowed parameters.

Both the homogeneous as well as the local stress scenario constrain the responsiveness G : a choice of G which is too low leads to a gradual increase of the duration of seed removal and then failure of seed removal. If G is too large, the repair times increase and eventually the tissue becomes unstable (see Figure 7A). Similarly, in the local stress scenario, if the focal range c becomes too large, then the tissue loses its focus and with it its ability to locally remove seeds, and transitions to the chronic state. Interestingly, strong local stressors introduce another constraint: if the focal range becomes too small, then the local stressor induces an instability. An elevated focal range, therefore, blurs out local subthreshold stressors and allows the tissue to remain functional (see Figure 7B). How do these limitations play out as stress levels increase?

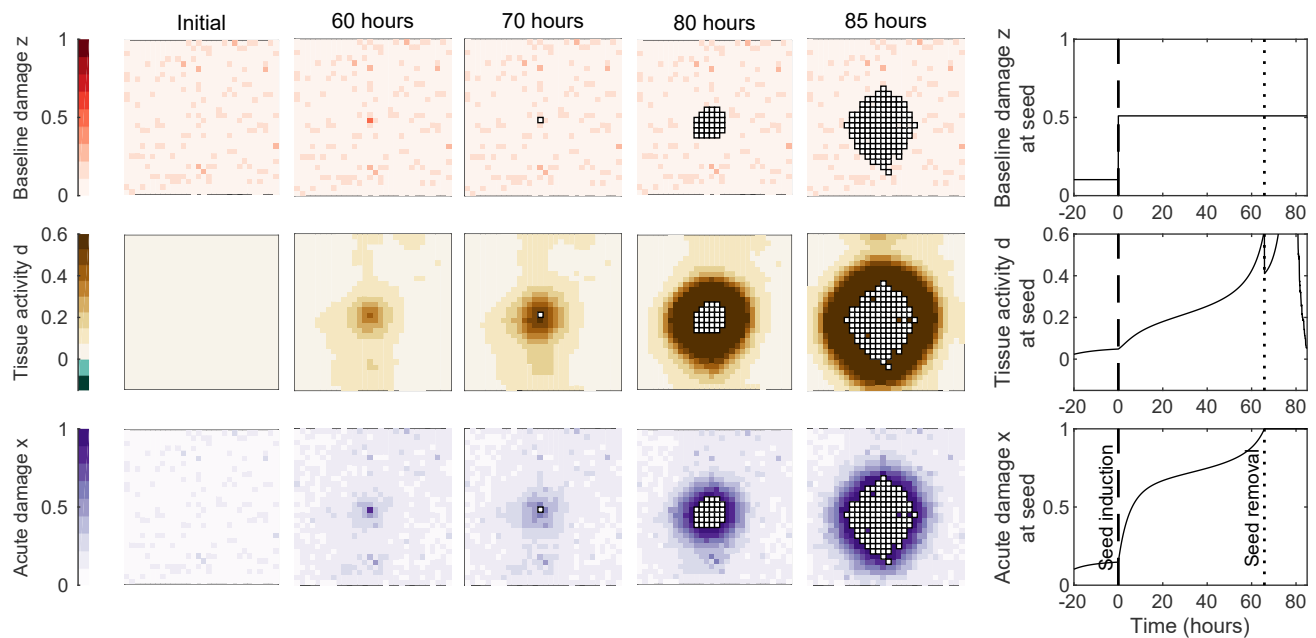


Figure 6. Primed Tissue State Leads to Acute Damage Propagation After Perturbation

Seed induction in a tissue with slightly elevated baseline damage $z = 0.075 \pm 0.035$, increased focal range $c = 0.55$, and high responsiveness $G = 3$ and attenuated protective reaction to cell death $D = 0$. Disposal of the seed is slow and affects surrounding tissue disproportionately. In contrast to Figure 4, seed removal does not successfully inhibit disposal-inducing effects. Instead, a domino-like spreading lesion is induced, with high levels of damage-inducing activity preceding the lesion front. See also Figures S3 and S4.

We studied the two aforementioned scenarios of homogeneous and local stressors, under increasing baseline damage (see Figure 8). The effect is dramatic—an increase in baseline damage z shifts the optimal set-point of the tissue, therefore requiring an adjustment of responsiveness and focal range. Also, the range of allowed parameters decreases, until it eventually becomes impossible to satisfy both the seed removal and the tissue stability conditions. An increase in baseline damage also means that even with an optimal adjustment of parameters, seed removal will still slow down and repair times will increase. Finally, a particularity of a local stressor is that the adjustment of the focal range can maintain stability. This adjustment comes with side effects such as increased reaction to subthreshold stress and possible damage propagation (see Figures 5 and 6).

In conclusion, reconciling seed removal and stability of the tissue increasingly restricts the parameter space as the baseline damage z increases. Maintenance of short- and long-term resilience therefore become conflicting goals for elevated baseline damage z levels.

DISCUSSION

We presented a model that describes repair and dispose decisions as a function of the tissue state. In order to validate the model, longitudinal studies of temporally and spatially highly resolved tissue properties for specific diseases, prior to disease onset, are needed. In the absence of this data, we compare how the model assumptions compare qualitatively with biological observations. Can the model indeed map some aspects of the progression of complex neurological diseases? We first discuss the experimental findings and the cellular mechanisms that motivated the fast repair and dispose model. We then discuss how the model captures slow disease-specific processes. In particular, we present a possible re-interpretation of stages for Alzheimer's disease (AD) and multiple sclerosis (MS), based on the model behavior.

The Role of Cellular Mechanisms in Seed Removal

Repair-or-Dispose

The model assumes the repair of cells with short-term-damage and disposal of highly damaged cells, as a tug-of-war between two opposing forces in the tissue. We suggest that glia-neuron crosstalk implements

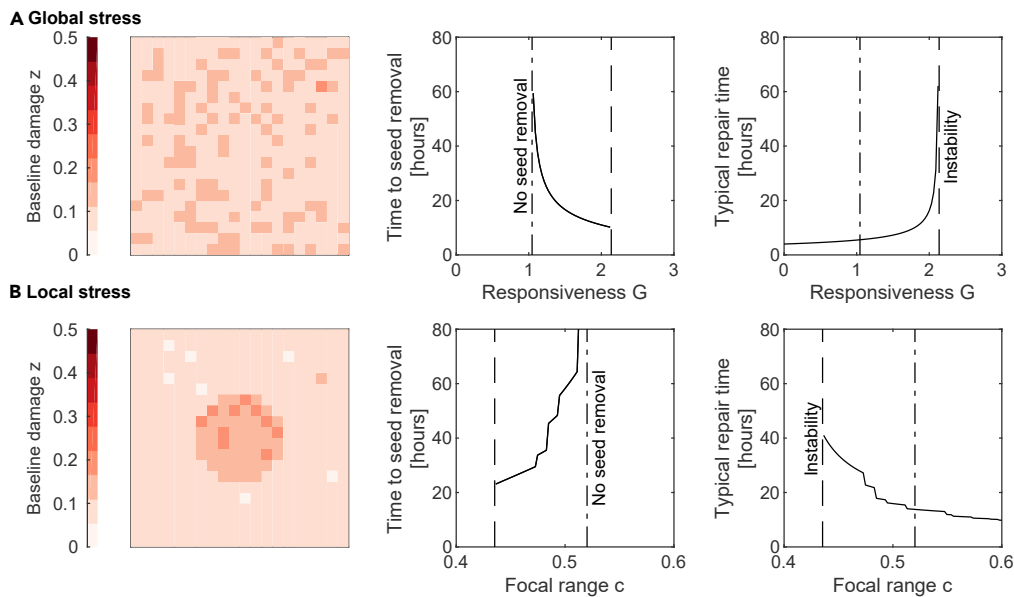


Figure 7. Transitions of Tissue Behavior

Behavior of tissue with homogeneous (A) and with locally constrained (B) baseline damage. We measure the time from seed induction to seed removal, as well as the typical timescale in which small perturbations are repaired. The latter measure is defined as the inverse of the maximal eigenvalue of the right hand side of Equation 2. Low responsiveness G leads to a failure of seed removal. In contrast, high responsiveness G leads to an increase of typical repair time, i.e. a reduced stability at the homeostatic set point. After crossing a critical value, the set point is lost, and self-damaging effects drive the cell population toward cell death. The corresponding parameter space is denoted by the term “instability.” For local stress scenarios, the focal range c can have a stabilizing effect and avoid instability. If values of c are too high, then seed removal breaks down. For A, the baseline damage is 0.1 ± 0.02 , and for B, the local baseline damage within the center region is $z = 0.15 \pm 0.02$ and otherwise $z = 0.075 \pm 0.02$.

such a bistable effect. Glia are the helper cells of the brain, and they maintain homeostasis and drive and resolve inflammation in the brain. The two most common glial cell types, microglia (Kreutzberg, 1996; Biber et al., 2007; Wolf et al., 2013; Kettenmann et al., 2011; Ransohoff, 2016) and astrocytes (Zamanian et al., 2012; Khakh and Sofroniew, 2015), exhibit differential and multidimensional activity patterns, which depend—among other factors—on the neuronal state. For instance, microglia provide neurotrophic support (Heneka et al., 2018) and surveil the tissue (Nimmerjahn et al., 2005). Microglial activity is suppressed by so-called neuronal “Off”-signals, which regulate sensing and housekeeping functions (Biber et al., 2007; Wolf et al., 2013; Kettenmann et al., 2011). These signals that induce repair are mediated by receptor-ligand interactions such as CX3CL1 and CD200 signaling (Hickman et al., 2018; Heneka et al., 2018).

Glial activation is, however, a double-edged sword and can, under certain conditions, induce neuronal damage (Czeh et al., 2011). For instance, neurons may directly recruit microglia by releasing ATP, facilitating phagocytosis (Harry, 2013), or by releasing glutamate, which triggers microglial tumor necrosis factor alpha (TNF- α) release (Kettenmann et al., 2011). Astrocytes respond to infections, trauma, or inflammation by reactive astrogliosis, characterized by an increased production of pro-inflammatory cytokines such as interleukin-1 β (IL-1 β) and TNF- α , and reactive oxygen species (ROS) (Sofroniew and Vinters, 2010). Overactivated microglia can induce the transition of nearby astrocytes to a highly neurotoxic phenotype, causing widespread damage to the tissue (Liddelow et al., 2017). Microglia can also remove stressed-but-viable neurons as a response to the “eat-me-signal” phosphatidylserine following elevated, but nontoxic, levels of glutamate, oxidative stress, or growth-factor withdrawal (Brown and Neher, 2010, 2014).

As a whole, these interactions between neurons and glia are high dimensional and involve a multitude of cell types and phenotypes. The model captures the aspect of these highly complex interactions that there exist two opposing net effects of glia-neuron crosstalk that are regulated by the neuronal damage. These effects are modeled by the bistable nature of the balance in Equation 2. The parameter G , which we call

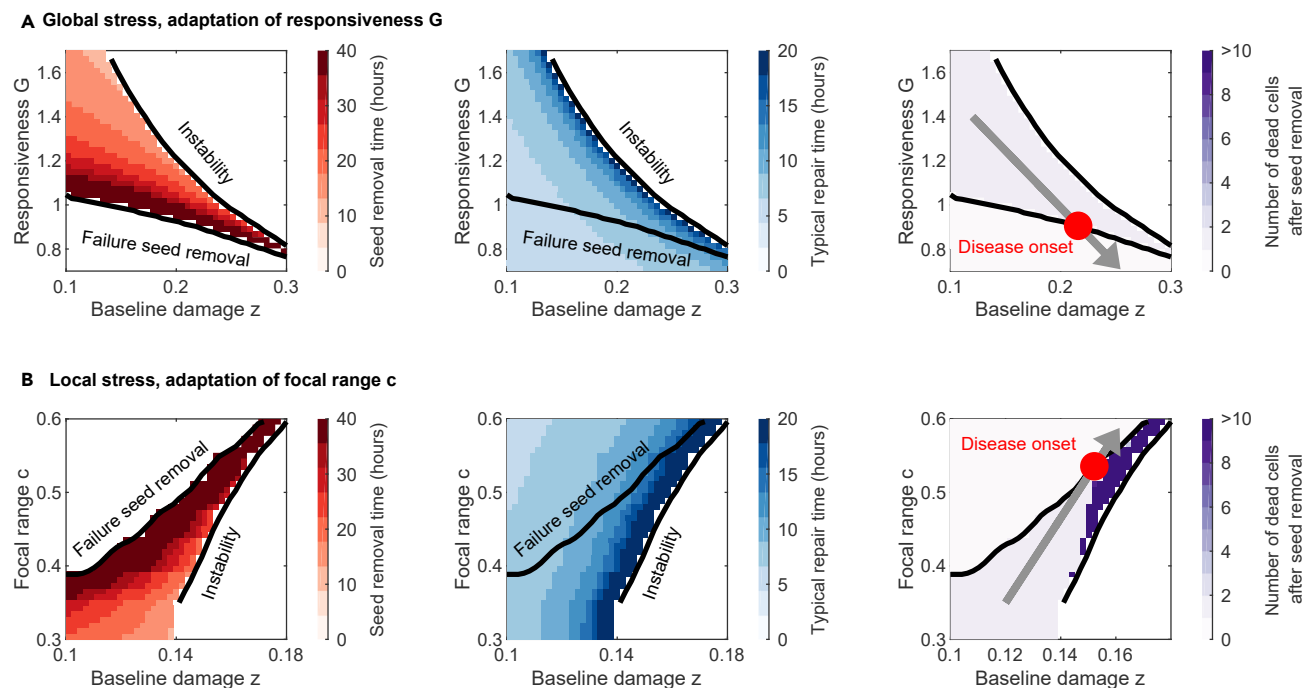


Figure 8. Tissue Adaptation to Increasing Baseline Damage z

Time between seed induction and seed removal (left column), typical repair time (center column), and number of dead cells after seed removal (right column). Transitions to instability and to failure of seed removal are defined by points at which repair time and seed removal times diverge, respectively. (A) Global stress scenario, with adaptation of responsiveness G for varying baseline stress levels z . (B) Local stress scenario, with adaptation of focal range c for varying baseline stress levels z . As the baseline damage increases, both the responsiveness G (left panel) as well as the focal range c (right panel) become increasingly constrained to avoid the loss of a stable set point (“instability”) and failure of seed removal. The plots on the right depict a possible course of tissue adaptation as baseline damage z increases. The point at which the seed removal fails marks the onset of slow degeneration (“disease onset”). Distribution of baseline damage as in Figure 7. See Figures S5 and S6 for a simulation with gradual adaptation of G and (C)

tissue responsiveness, describes how readily dispose-inducing effects are activated. Therefore, a sufficiently high value of G describes that cellular communication is intact.

Spatial Effects

The model also assumes that glia do not act perfectly precise in space and may therefore affect neighboring parts of the tissue. This can happen through different pathways: for instance, proinflammatory phenotypes in neighboring cells can be induced by cytokine diffusion. Microglia migrate to regions of neural injury (Stence et al., 2001; Tønnesen et al., 2018) and form clusters as a reaction to blood-derived fibrinogen (Davalos et al., 2012). Therefore, inhibition of microglial motility (Damani et al., 2011) can lead to a loss of specificity and loss of precision. Also, astrocytic gap junction communication has been shown to play a role in spatial propagation of cell injury (Lin et al., 1998) and neuroprotection in ischemia (Nakase et al., 2003; Lin et al., 2008) (see (Giaume et al., 2010) for a review). Any inhibition or dysregulation of these spatial effects is modeled by an elevation of parameter c in Equation 3.

Glial Reactions to Cell Death

An important component of seed removal is the downregulation of disposal-inducing effects after seed removal, i.e. after cell death. This assumption is supported by several observations. Cell death and phagocytosis is a highly complex and heterogeneous process (Elliott and Ravichandran, 2016). In this process, microglia clear neuronal debris (Kreutzberg, 1996), secrete anti-inflammatory cytokines, and minimize damage to surrounding cells (Savill and Fadok, 2000; Elmore, 2007; Broughton et al., 2009). These protective effects are captured by negative values of the parameter D in Equation 4. It is not fully clear how long this process takes. However, “phagocytic ingestion” was reported to take from 15 up to 160 min (Petersen and Dailey, 2004; Witting et al., 2000). After engulfment, the apoptotic cargo must then be processed

(Arandjelovic and Ravichandran, 2015). In our simulations, we therefore assume that the process from detection of the apoptotic cell, engulfment, to processing of the cargo is defined by the timescale of one day.

The reaction to cell death can be disturbed in several ways. For example, it was shown that an epigenetically mediated dysregulation of the tightly controlled clearance function can lead to damage in healthy neurons (Ayata et al., 2018). Also following necrosis (Poon et al., 2014), in age (Neumann et al., 2008), and in neurodegenerative diseases (Napoli and Neumann, 2009), phagocytosis is reduced or can induce pro-inflammatory reactions via ATP released from dying neurons (Di Virgilio et al., 2009). In particular, necrosis can have detrimental effects on neighboring cells. It is characterized by a loss of cell membrane integrity and the uncontrolled release of cell products into the extracellular matrix following acute cellular injury caused by external toxic factors such as TNF- α . A programmed form of necrosis is necroptosis, also dubbed “cellular suicide.” In MS, oligodendrocytes have been found to undergo necroptosis (Ofengeim et al., 2015). In AD, neuronal loss due to necroptosis has recently been reported (Caccamo et al., 2017). The net detrimental effects of cell death to the surrounding tissue is captured by higher levels of D . The model computations predict acute lesion spread as a possible outcome (see Figure 6).

Neurodegenerative Disease Progression

The model predicts the resilience of a self-cleaning tissue under stress. This situation is found in many neurodegenerative diseases: the self-cleaning properties of glia-neuron crosstalk are put under stress by amyloid accumulation, immune attacks from the periphery, and cardiovascular stress. In parallel to these effects that strain glia-neuron crosstalk, the drivers of neurodegeneration are included as slow processes that typically operate on the timescale of months to years: The accumulation of nonrepairable baseline damage such as intracellular tau accumulation (Gan et al., 2018) or permanent demyelination (Mahad et al., 2015) are represented by the variable z . The increase and spread of this damage is represented by the number of M cells the damage spreads to (see also Sec. S4). The spread could be via intracellular “protein condensation” (Shin and Brangwynne, 2017; Fu et al., 2018), self-propagating protein assemblies (Venegas et al., 2017; Jucker and Walker, 2018), and the vicious cycle of deleterious inflammation and neurodegeneration (Block et al., 2007; Yuan et al., 2018). As shown in Figure 8, the model predicts warning signs that precede the breakdown of functional glia-neuron crosstalk and the take-over of slow neurodegenerative damage spread. In this section, we explore these analogies to the disease courses of AD and MS (see Figure 9). We postulate that there are common system-level mechanisms that precede the clinical outbreak of the diseases. We note that these mechanisms exhibit similarities to processes in tumor development. For example, most clinically detected cancers must have evaded system-mediated immune responses (Gajewski et al., 2013), and pre-treatment tumor T cell signatures can predict clinical responses to therapy (Jiang et al., 2018). The importance of the initial tumor microenvironment for the “turning point,” i.e. the development of an exponentially growing tumor is reminiscent of the dependence of the onset of neurodegeneration on glia-neuron crosstalk that we describe here for neurological diseases.

Alzheimer Disease

AD is a neurodegenerative disease characterized by the extracellular accumulation of amyloid- β (A β) plaques, as well as intracellular accumulation of neurofibrillary tangles consisting of misfolded, hyperphosphorylated tau protein (Henstridge et al., 2019). Next to genetic risk factors (Karch and Goate, 2015), also lifestyle, cardiovascular disease (Santos et al., 2017), and meningeal glymphatic system dysfunction (Da Mesquita et al., 2018) contribute to disease outbreak. It is thought that seeds recruit their soluble counterparts in living cells, therefore establishing a self-driven process. There is also evidence that neurodegeneration and glial reaction to it form a positive feedback (Block and Hong, 2005; Block et al., 2007).

In vitro studies for AD show that A β induces inflammatory microglial responses (Halle et al., 2008; Sheedy et al., 2013) and primes microglia for a secondary stimulus (Heppner et al., 2015). These activated glial cells appear before the first structural changes in the tissue (Heneka et al., 2015a). In the early stages of aggregation the immune response amplifies the glial clearance abilities (Heneka et al., 2015b). However, prolonged exposure to excessive concentrations of proteins causes chronic inflammation. Overactivated microglia and reactive astrocytes then express neurotoxic factors (Gold and El Khoury, 2015; El Khoury et al., 2003; Coraci et al., 2002) and impaired A β clearance (Von Bernhardi et al., 2015) and lose their cleaning abilities (Spangenberg et al., 2016). This winds up the protein aggregation (De Strooper and Karran, 2016) and compromises the inflammation resilience in a vicious feedback loop. In AD, the feedback has recently been

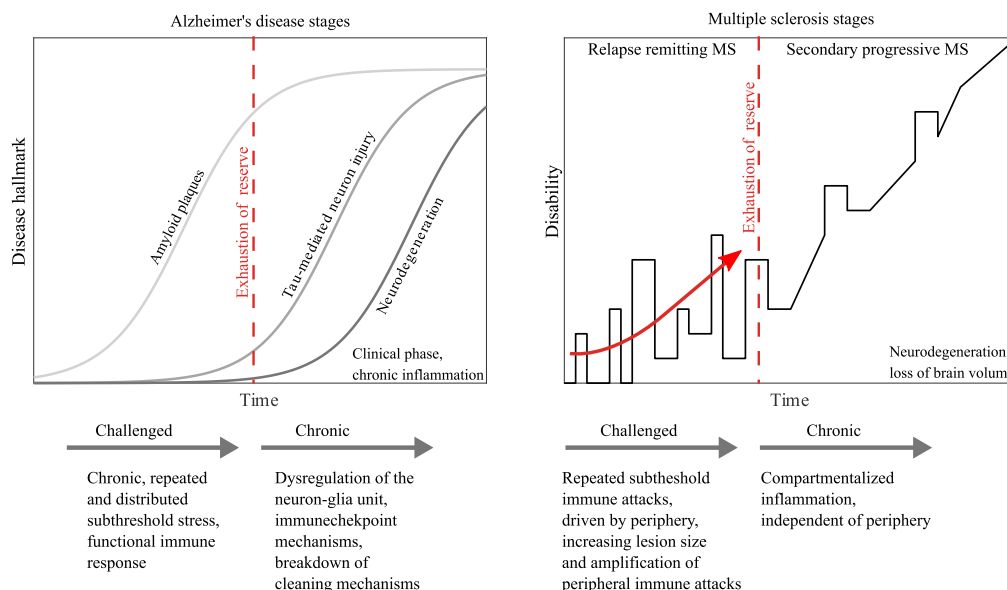


Figure 9. Suggested Disease-Model Analogy

(Left) Stereotypical stages of AD disease progression: Amyloid plaque deposition can be viewed as chronic distributed stress on the tissue, which leads to a slow adaptation. Once the reserve of this phase is exhausted, self-cleaning mechanisms break down, allowing for the spread of baseline damage, e.g. via tau-mediated neuronal injury. Only in the final phase is an increase in cell death observed. The model suggests that the breakdown of the glia-neuron unit and of functional immune responses are at the core of the transition from the challenged to the chronic and final neurodegenerative phase. (Right) Stereotypical stages of MS disease progression: repeated local immune attacks, driven by the periphery, are analogous to local stressors. As the limit of adaptation is approached, the effect and lesion sizes of peripheral immune attack increase (see red arrow). Breakdown of functional immune responses signals the transition from relapse-remitting MS to secondary progressive MS, i.e. the transition to the chronic phase, characterized by compartmentalization, self-driven neurodegeneration, and chronic dysfunctional inflammation.

linked to microglia- and inflammation-driven cross-seeding for A β pathology (Venegas et al., 2017). These processes extend the “amyloid cascade hypothesis,” where A β is seen as the main driving force of the disease. In particular, it has been proposed that AD transitions from a reversible disease course to an irreversible chronic autonomous cellular response. In this phase, disease progression no longer depends on aggregated proteins that trigger the initial response but on glial chronic inflammation (Von Bernhardi, 2007; De Strooper and Karran, 2016). We therefore include A β pathology as a baseline damage in our model, from which a dysregulated tissue response and failed removal of seeds ensues.

Several aspects of the role of glia-neuron crosstalk for AD progression are captured by the model proposed in this work. First, the affinity of a tissue to induce intracellular misfolded tau protein is represented by the rate with which seeds are induced. Low subthreshold stressors such as lifestyle, glymphatic system dysfunction, and amyloid plaque accumulation correspond to weak distributed frequent stressors on the tissue, which elevate baseline damage levels (z) (see Figures 7 and 8). In addition, there is evidence that misfolded proteins, in particular tau and α -synuclein, can propagate from neuron to neuron (De Calignon et al., 2012; Brettschneider et al., 2015; Surmeier et al., 2017; Vogel et al., 2020; Uemura et al., 2020) in a “prion-like” manner (Jucker and Walker, 2018). This self-propagating seeding process may spread via synaptic connections (De Calignon et al., 2012; Guo and Lee, 2014; Vogel et al., 2020) or other mechanisms (Brettschneider et al., 2015), corresponding to spread of baseline damage. Another process through which the disease could spread is network dysfunction, in particular amyloid-dependent hyperexcitability of neurons with baseline activity, setting off a vicious circle of increasing neuronal activity (Busche et al., 2008; Zott et al., 2019).

The model computations in Figure 8 show how the slow accumulation of subthreshold baseline damage requires an adaptation of responsiveness G and eventually leads to the breakdown of self-cleaning, i.e. the ability to react to intracellular tau. After breakdown of self-cleaning, the system transitions from the

challenged to the chronic phase, with first an accumulation of neuronal damage and an increase in seeds (increase in tau and further increase of amyloid), and finally neuronal loss, which is in line with the typical time course of AD (see [Figure 9](#)).

The implication of adaptive self-cleaning processes in the breakdown of resilience is in line with recent genetic studies. In particular, they implicate mutations in genes expressed by immune-active cells in the development of late-onset AD—one major risk factor being a mutation of TREM2 (triggering receptor expressed on myeloid cells 2) ([Hickman et al., 2018](#)). TREM2 encodes an innate immune receptor expressed by microglia and is part of an immune checkpoint that controls the activation of A β -clearing disease-associated microglia. In particular, functional TREM2 leads to an upregulated microglial phagocytosis of A β plaques early in the disease by activated microglia, but it also increases levels of ApoE (plaque-associated apolipoprotein E) in A β plaques, which promotes misfolded protein aggregation ([Parhizkar et al., 2019](#); [Henstridge et al., 2019](#))—analogous to the ambiguous role of tissue responsiveness *G* in the model. In contrast, TREM2 loss-of-function mice exhibit microglia that appear to be locked in a homeostatic state ([Parhizkar et al., 2019](#); [Song et al., 2018](#); [Hickman et al., 2018](#)). This promotes plaque growth early but not late in the disease. This means that intriguingly, the function of TREM2 signaling is analogous to the responsiveness *G* in the model—it participates in active seed removal in healthy tissue but is counterproductive in the chronic phase.

This hints at a possible transition from a challenged but functional phase to a chronic phase, corresponding to the so-called cellular phase, in which clearance mechanisms break down ([De Strooper and Karran, 2016](#)). Once the chronic phase is entered, several slow neurodegenerative processes drive disease progression. For instance, dying or damaged neurons release so-called danger-associated molecular patterns (DAMPs). These can initiate microglial NLRP3 inflammasome activation, enhance amyloid seeding, and promote tau hyperphosphorylation ([Hickman et al., 2018](#); [Heneka et al., 2018](#)). Experiments also indicate that A β plaques disseminate throughout the brain, even though the underlying mechanisms are not yet fully understood ([Jucker and Walker, 2018](#)).

Importantly, the model suggests that the transition to the chronic phase is a self-protective measure: Consider a situation in which stress on neurons with a selective vulnerability to protein aggregation ([Fu et al., 2018](#)) becomes excessive, or if average damage levels are too high, e.g. due to cardiovascular disease. In this case of high baseline damage *z*, an active removal of seeds can induce collateral damage and becomes counter-productive (see [Figure 6](#)). The model suggests that downregulation of glial responsiveness *G*, which compromises long-term resilience at the benefit of maintaining short-term resilience, is then the lesser of two evils. Similarly, the intracellular accumulation of misfolded proteins in AD (and also in Parkinson disease), influences glial reactions to cell-death *D*. Glial phagocytic function may become upregulated and negatively affect neighboring neurons ([Ayata et al., 2018](#)); and necrosis of long-term stressed neurons can lead to further inflammation and damage propagation ([Yuan et al., 2018](#)). This can lead to fast domino-like passing on of neurodegeneration to neighboring tissue, characteristic for the primed state (see [Figure 6](#)).

In summary, the model computations suggest that amyloid plaque accumulation, together with other factors, gradually increase baseline damage. This leads to a challenged tissue state, in which in order to maintain short-term stability, the tissue continuously lowers its responsiveness. Once the reserve of this state is exhausted, self-cleaning mechanisms of glia-neuron crosstalk break down, allowing for a spread of tau-mediated neuron-injury (baseline damage). Only in the final stage, neuron death is observed.

Multiple Sclerosis

A hallmark feature of MS is that immune cells penetrate the brain, demyelinate neurons ([Lublin et al., 2014](#)), and induce excitotoxic insults ([Siffrin et al., 2010](#); [Liblau et al., 2013](#)). MS often progresses in two sequential disease phases ([Mahad et al., 2015](#)). In the first phase, also referred to as relapse-remitting MS (RRMS), neurodegeneration is driven by immune cells entering the CNS from the periphery through the blood-brain-barrier and attacking myelin sheaths and axons. In the second phase, also referred to as secondary progressive phase (SPMS), neurodegeneration is compartmentalized and chronic. The transition point between these two phases is highly patient specific and may either happen within a few months, decades, or, as in some patients, not occur at all. The reasons for the transition and

its high variability are not fully understood (Larochelle et al., 2016). So, are there slow self-propagating mechanisms in MS?

We identify several self-propagating processes that can induce a vicious neurodegenerative cycle and which correspond to the slow propagation of baseline damage in the model. (1) First, in acute MS lesions, the transporter protein levels GLT-1 and GLAST are dysregulated and therefore impaired in their ability to take up glutamate (Korn et al., 2005; Mitosek-Szewczyk et al., 2008). This is also seen in amyotrophic lateral sclerosis (ALS) (Maragakis and Rothstein, 2006). This reduction in the astrocytic glutamate uptake (Petr et al., 2015) can exacerbate the toxic increases of intracellular calcium (Luchtman et al., 2016) following T cell attacks in MS. This means that the tissue becomes increasingly vulnerable to excitotoxicity and external stress. (2) Second, in age and in disease, glial processes can reduce remyelination of neuronal axons. This may be a consequence of impaired myelin clearance from an initial injury due to reduced motility, surveillance, and phagocytic activity of activated microglia with age (Rawji et al., 2018). In MS, impaired myelin debris clearance can then lead to cholesterol crystallization, inflammasome activation, and a maladaptive immune response (Cantuti-Castelvetri et al., 2018; Franklin and ffrench-Constant, 2017). Importantly, reduced myelin debris clearance, and the resulting myelin debris in the tissue, inhibits oligodendrocyte progenitor cell differentiation into oligodendrocytes (Franklin and ffrench-Constant, 2017), further aggravating the problem. (3) Third, in MS, regulatory lymphocytes, which act through crosstalk with microglia (El Behi et al., 2017), are less effective in inducing remyelination. Also, chronic inflammation and microglial activation, and increasing neuronal oxidative stress and damage of the axon-glia unit, can lead to a self-perpetuating vicious cycle (Hemmer et al., 2015; Nave, 2010). Recent studies even point at the possibility that decoupled pathological protein-propagation contributes to this vicious cycle in progressive MS, although research is still at an early stage (Schattling et al., 2019).

Apart from the self-perpetuating procyclic effects described earlier, the model captures the local nature of repeated immune attacks around blood vessels as local increase in baseline damage z (see Figures 7 and 8). Permanent demyelination of neurons is captured by the baseline damage z , and reversible demyelination and abnormal intracellular calcium elevations are represented by acute damage variable x . The tissue reaction to damaged neurons is captured by the parameter G . As the disease progresses, the repeated immune attacks increasingly put the responsiveness of immune competent cells to the test: glial responsiveness to immune attacks can cause collateral damage to neighboring cells but is needed for repair and maintenance, to avoid neurodegenerative processes. The model suggests that in order to avoid a breakdown of short-term stability and collateral damage by acute lesion spread, the focal range c is increased. The side effect is a less stable tissue, in which the “footprint” of immune attacks increases. The increased susceptibility is reminiscent of the increasing intensity of RRMS lesions before the transition to SPMS. In the extreme case, the acute lesion spread described in Figure 6 is similar to the development of quickly expanding lesions in fulminant MS (Rohani and Ghourchian, 2011). Eventually, the adaptation to high baseline levels leads to a breakdown of seed removal—this means the removal of highly demyelinated neurons ceases, which allows for the development of slow neurodegenerative processes. Slow compartmentalized neurodegenerative processes take over, leading to a transition to the chronic phase (see also Table 1). The model therefore suggests that the point at which focal range c is increased and glial responsiveness G is downregulated so much that seed removal breaks down characterizes the transition from RRMS to SPMS. Postponing the transition from RRMS to SPMS therefore hinges on the careful management of immune attacks and subsequent tissue adaptation.

Conclusion

The key result of our model computation is that maintenance of seed removal and short-term resilience become conflicting goals with increasing tissue damage. This is consistent with features of disease progression in AD and MS. Therefore, even though evidence suggests that overlap of genetic susceptibility between neurodegenerative (De Jager et al., 2018) and neuroinflammatory (Filiou et al., 2014) diseases is low, our model hints at the possibility of common system-level mechanisms, which precede the clinical outbreak of the diseases. So, how could a transition from a functional tissue to a primed (failure of short-term resilience) or chronic (failure of long-term resilience) be postponed? Possible targets are (1) maintenance of the active elements of self-cleaning, i.e. responsiveness G and focal range c ; (2) maintenance of reaction to cell death (D); and (3) minimization of long-term subthreshold stressors that lead to an increase of baseline damage z .

To maintain the self-cleaning mechanism, responsiveness G needs to stay high and focal range c low. Possible avenues to do this are the maintenance of the various checkpoint mechanisms of the innate immune system (Deczkowska et al., 2018), as well maintenance of microglial motility (Damani et al., 2011). Both become dysregulated in age (Nativio et al., 2018). Warning signs that signal the exhaustion of the challenged state, and a possible failure of self-cleaning, are slowed responsiveness, delayed seed removal (see Figures 5A and 8), and decreased short-term stability (see Figures 6 and 8). The model therefore suggests that changes of the dynamic tissue reaction to focal stress predict disease onset.

This constitutes the model prediction to be tested: disease onset coincides with the breakdown of a glia-neuron control mechanism that upregulates tissue activity following injury and that the breakdown is preceded by two opposing observations: (1) small, repairable injuries are resolved at a slower rate (see repair time in Figure 8), and (2) injury that requires an inflammatory response (seed removal) take longer to initiate that necessary tissue response (see “time to seed removal” in Figure 8). The disease onset coincides with breakdown of (2), i.e the ability to cause adequate tissue responses. Confirming or refuting this process hinges on the development of biomarkers for the dynamic tissue response to physiologically small and focused injury (seed inductions). If confirmed, this could be a potential diagnostic tool. Note that in contrast to early disease phases, in which high responsiveness G needs to be maintained, our results show that in the chronic phase, active seed removal is dysfunctional, calling for a downregulation of responsiveness G , e.g. using anti-inflammatory treatments. This decreases the risk of collateral damage (see Figure 6) and slows down feedback processes that drive neurodegeneration. Furthermore, an anti-inflammatory protective tissue reaction to cell death is required (negative D). The exhaustion of this effect may lead to a primed state and therefore act as an accelerator and facilitator of neurological disease progression, in particular in protein-accumulating diseases. To avoid or postpone this transition, therapeutic interventions need to selectively reinforce the resolution of glial responsiveness after cell death.

In conclusion, we propose a self-consistent computational description of a self-cleaning mechanism under stress with a minimal number of parameters. Analysis and model computations suggest the existence of four stereotypical tissue states and a typical pattern for disease progression, dependent on the stressor. The ingredients of the model reflect several key properties of glia-neuron crosstalk and model predictions match current genetic and experimental findings for two of the most common neurodegenerative conditions. Mechanistically, the model suggests the following state-specific interventions: maintenance of glial fitness, responsiveness, and focal range in early, pre-clinical phases; management of the ability to contain and resolve glial activation after cell death; and reduction of responsiveness in the chronic phase of the disease. Specifically, the model suggests how a failure to consolidate short- and long-term resilience might be at the heart of the onset of common neurological diseases.

Limitations of the Study

Here, we put forward a reductionist model to generate a hypothesis about the transition between neurodegenerative disease stages. The abstract nature of the model means that it does not represent the complexity of the biology and disease progression. Instead, it focuses on one specific aspect—the interaction between a fast repair-and-dispose mechanism and slow degeneration. For example, the model uses one-dimensional abstract measure for baseline and acute damage z and x to capture the transitions between tissue states. These damage measures are compositions of a high-dimensional space of cellular properties and differ from disease to disease. The damage quantities x and z , therefore, do not represent the full health of the cell but only the one-dimensional projection that is relevant to the specific aspect modeled in this study. Understanding which measurable quantities x and z are composed of constitutes a challenge, which is outside of the scope of this study.

The results presented here, and the comparison with neurodegenerative diseases, do not constitute a proof or validation that the transition between disease states are driven by the mechanisms described here. Instead, these results present a plausible hypothesis, which needs to be tied to specific pathologies and the underlying mechanisms in order to be validated. In particular, the model can be predictive once the parameters can be understood and estimated from the experimental data. For instance, in order to validate the hypothesis put forward in this work, temporally and spatially highly resolved biomarkers for glial and inflammatory activation, as well as for neuronal damage, need to be measured prior to onset of clinical disease in humans in a longitudinal study.

Resource Availability

Lead Contact

Further information and requests for resources and reagents should be directed to and will be fulfilled by the Lead Contact, Andreas Nold (andreasnold@me.com).

Materials Availability

This study did not generate new unique reagents.

Data and Code Availability

The code used to generate the results presented in this study is available on <https://gitlab.mpcdf.mpg.de/mpibrano/resiliencefastandslow>.

METHODS

All methods can be found in the accompanying [Transparent Methods supplemental file](#).

SUPPLEMENTAL INFORMATION

Supplemental Information can be found online at <https://doi.org/10.1016/j.isci.2020.101701>.

ACKNOWLEDGMENTS

This study was supported by the Max Planck Society (T.T.), German Research Foundation (DFG, SFB CRC-TR-128 to S.B.), the Hertie foundation (mylab, S.B.), the Joachim Herz Foundation (Add-on fellowship, A.N.), the German Academic Exchange Service (DAAD-scholarship, D.B.), the International Max Planck Research School for Neural Circuits (IMPRS, D.B.) and the Center for Personalized Translational Epilepsy Research (CePTER funding, D.B.). The authors are members of the Rhine-Main Neuroscience Network (rmn2). We thank Jochen Roeper and Olga Garaschuk for their insights into possible roles of the mechanism in Parkinson's and Alzheimer's diseases, respectively. A.N. thanks Tatiana Engel for stimulating discussions about the model framework and Daniela Swardt for proofreading the manuscript.

AUTHOR CONTRIBUTIONS

A.N., D.B., K.B., S.B., and T.T. conceived the study; A.N. and D.B. performed the research; A.N. conducted the mathematical analysis and prepared the first draft of the manuscript, A.N., S.B., and T.T. wrote the manuscript, and all authors revised the final manuscript.

DECLARATION OF INTERESTS

Stefan Bittner has received Honoraria and compensation for travel from Biogen Idec, Merck Serono, Novartis, Sanofi-Genzyme, and Roche. Katharina Birkner is an employee of AbbVie Inc.

Received: February 7, 2020

Revised: July 17, 2020

Accepted: October 15, 2020

Published: November 20, 2020

REFERENCES

- Abboud, A., Mi, Q., Puccio, A., Okonkwo, D., Buliga, M., Constantine, G., and Vodovotz, Y. (2016). Inflammation following traumatic brain injury in humans: insights from data-driven and mechanistic models into survival and death. *Front. Pharmacol.* *7*, 342.
- Aguzzi, A., Barres, B.A., and Bennett, M.L. (2013). Microglia: scapegoat, saboteur, or something else? *Science* *339*, 156–161.
- Anderson, W.D., and Vadigepalli, R. (2016). Modeling cytokine regulatory network dynamics driving neuroinflammation in central nervous system disorders. *Drug Discov. Today Dis. Models* *19*, 59–67.
- Arandjelovic, S., and Ravichandran, K.S. (2015). Phagocytosis of apoptotic cells in homeostasis. *Nat. Immunol.* *16*, 907–917.
- Ayata, P., Badimon, A., Strasburger, H.J., Duff, M.K., Montgomery, S.E., Loh, Y.H.E., Ebert, A., Pimenova, A.A., Ramirez, B.R., Chan, A.T., et al. (2018). Epigenetic regulation of brain region-specific microglia clearance activity. *Nat. Neurosci.* *21*, 1049.
- Barres, B.A. (2008). The mystery and magic of glia: a perspective on their roles in health and disease. *Neuron* *60*, 430–440.
- Biber, K., Neumann, H., Inoue, K., and Boddeke, H.W. (2007). Neuronal 'on' and 'off' signals control microglia. *Trends Neurosci.* *30*, 596–602.
- Block, M.L., and Hong, J.S. (2005). Microglia and inflammation-mediated neurodegeneration: multiple triggers with a common mechanism. *Prog. Neurobiol.* *76*, 77–98.
- Block, M.L., Zecca, L., and Hong, J.S. (2007). Microglia-mediated neurotoxicity: uncovering

the molecular mechanisms. *Nat. Rev. Neurosci.* 8, 57.

Brettschneider, J., Del Tredici, K., Lee, V.M.Y., and Trojanowski, J.Q. (2015). Spreading of pathology in neurodegenerative diseases: a focus on human studies. *Nat. Rev. Neurosci.* 16, 109–120.

Broughton, B.R.S., Reutens, D.C., and Sobey, C.G. (2009). Apoptotic mechanisms after cerebral ischemia. *Stroke* 40, e331–e339.

Brown, G.C., and Neher, J.J. (2010). Inflammatory neurodegeneration and mechanisms of microglial killing of neurons. *Mol. Neurobiol.* 41, 242–247.

Brown, G.C., and Neher, J.J. (2014). Microglial phagocytosis of live neurons. *Nat. Rev. Neurosci.* 15, 209–216.

Busche, M.A., Eichhoff, G., Adelsberger, H., Abramowski, D., Wiederhold, K.H., Haass, C., Staufenbiel, M., Konnerth, A., and Garaschuk, O. (2008). Clusters of hyperactive neurons near amyloid plaques in a mouse model of Alzheimer's disease. *Science* 321, 1686–1689.

Caccamo, A., Branca, C., Piras, I.S., Ferreira, E., Huentelman, M.J., Liang, W.S., Readhead, B., Dudley, J.T., Spangenberg, E.E., Green, K.N., et al. (2017). Necroptosis activation in Alzheimer's disease. *Nat. Neurosci.* 20, 1236–1246.

Cantuti-Castelvetri, L., Fitzner, D., Bosch-Queralt, M., Weil, M.T., Su, M., Sen, P., Ruhwedel, T., Mitkovski, M., Trendelenburg, G., Lütjohann, D., et al. (2018). Defective cholesterol clearance limits remyelination in the aged central nervous system. *Science* 359, 684–688.

Chizhov, A.V., Zefirov, A.V., Amakhin, D.V., Smirnova, E.Y., and Zaitsev, A.V. (2018). Minimal model of interictal and ictal discharges “epileptor-2”. *PLoS Comput. Biol.* 14, e1006186.

Cloutier, M., Bolger, F.B., Lowry, J.P., and Wellstead, P. (2009). An integrative dynamic model of brain energy metabolism using in vivo neurochemical measurements. *J. Comput. Neurosci.* 27, 391.

Cloutier, M., and Wellstead, P. (2012). Dynamic modelling of protein and oxidative metabolisms simulates the pathogenesis of Parkinson's disease. *IET Syst. Biol.* 6, 65–72.

Constantine, G., Buliga, M., Mi, Q., Constantine, F., Abboud, A., Zamora, R., Puccio, A., Okonkwo, D., and Vodovotz, Y. (2016). Dynamic profiling: modeling the dynamics of inflammation and predicting outcomes in traumatic brain injury patients. *Front. Pharmacol.* 7, 383.

Coraci, I.S., Husemann, J., Berman, J.W., Hulette, C., Dufour, J.H., Campanella, G.K., Luster, A.D., Silverstein, S.C., and El Khoury, J.B. (2002). CD36, a class B scavenger receptor, is expressed on microglia in Alzheimer's disease brains and can mediate production of reactive oxygen species in response to β -amyloid fibrils. *Am. J. Pathol.* 160, 101–112.

Czeh, M., Gressens, P., and Kaindl, A.M. (2011). The yin and yang of microglia. *Dev. Neurosci.* 33, 199–209.

Da Mesquita, S., Louveau, A., Vaccari, A., Smirnov, I., Cornelison, R.C., Kingsmore, K.M., Contarino, C., Onengut-Gumuscu, S., Farber, E., Raper, D., et al. (2018). Functional aspects of meningeal lymphatics in ageing and Alzheimer's disease. *Nature* 560, 185–191.

Damani, M.R., Zhao, L., Fontainhas, A.M., Amaral, J., Fariss, R.N., and Wong, W.T. (2011). Age-related alterations in the dynamic behavior of microglia. *Aging Cell* 10, 263–276.

Davalos, D., Ryu, J.K., Merlini, M., Baeten, K.M., Le Moan, N., Petersen, M.A., Deerinck, T.J., Smirnov, D.S., Bedard, C., Hakozaki, H., et al. (2012). Fibrinogen-induced perivascular microglial clustering is required for the development of axonal damage in neuroinflammation. *Nat. Commun.* 3, 1227.

De Calignon, A., Polydoro, M., Suárez-Calvet, M., William, C., Adamowicz, D.H., Kopeikina, K.J., Pitstick, R., Sahara, N., Ashe, K.H., Carlson, G.A., et al. (2012). Propagation of tau pathology in a model of early Alzheimer's disease. *Neuron* 73, 685–697.

De Jager, P.L., Yang, H.S., and Bennett, D.A. (2018). Deconstructing and targeting the genomic architecture of human neurodegeneration. *Nat. Neurosci.* 21, 1310.

De Strooper, B., and Karran, E. (2016). The cellular phase of Alzheimer's disease. *Cell* 164, 603–615.

Deczkowska, A., Amit, I., and Schwartz, M. (2018). Microglial immune checkpoint mechanisms. *Nat. Neurosci.* 21, 779–786.

Di Virgilio, F., Ceruti, S., Bramanti, P., and Abbracchio, M.P. (2009). Purinergic signalling in inflammation of the central nervous system. *Trends Neurosci.* 32, 79–87.

El Behi, M., Sanson, C., Bachelin, C., Guillot-Noël, L., Fransson, J., Stankoff, B., Maillart, E., Sarrazin, N., Guillemot, V., Abdi, H., et al. (2017). Adaptive human immunity drives remyelination in a mouse model of demyelination. *Brain* 140, 967–980.

El Houssaini, K., Bernard, C., and Jirsa, V.K. (2019). The epileptor model: a systematic mathematical analysis linked to the dynamics of seizures, refractory status epilepticus and depolarization block. *Eneuro* 7, 0485-18, <https://doi.org/10.1523/ENEURO.0485-18.2019>.

El Khoury, J.B., Moore, K.J., Means, T.K., Leung, J., Terada, K., Toft, M., Freeman, M.W., and Luster, A.D. (2003). CD36 mediates the innate host response to β -amyloid. *J. Exp. Med.* 197, 1657–1666.

Elliott, M.R., and Ravichandran, K.S. (2016). The dynamics of apoptotic cell clearance. *Dev. Cell* 38, 147–160.

Elmore, S. (2007). Apoptosis: a review of programmed cell death. *Toxicol. Pathol.* 35, 495–516.

Filiou, M.D., Arefin, A.S., Moscato, P., and Graeber, M.B. (2014). Neuroinflammation' differs categorically from inflammation: transcriptomes of Alzheimer's disease, Parkinson's disease, schizophrenia and inflammatory diseases compared. *Neurogenetics* 15, 201–212.

Franklin, R.J., and ffrench-Constant, C. (2017). Regenerating CNS myelin: from mechanisms to experimental medicines. *Nat. Rev. Neurosci.* 18, 753, <https://doi.org/10.1038/nrn.2017.136>.

Fu, H., Hardy, J., and Duff, K.E. (2018). Selective vulnerability in neurodegenerative diseases. *Nat. Neurosci.* 21, 1350–1358.

Fussenegger, M., Bailey, J.E., and Varner, J. (2000). A mathematical model of caspase function in apoptosis. *Nat. Biotechnol.* 18, 768–774.

Gajewski, T.F., Schreiber, H., and Fu, Y.X. (2013). Innate and adaptive immune cells in the tumor microenvironment. *Nat. Immunol.* 14, 1014–1022.

Gan, L., Cookson, M.R., Petrucelli, L., and La Spada, A.R. (2018). Converging pathways in neurodegeneration, from genetics to mechanisms. *Nat. Neurosci.* 21, 1300.

Garg, P., and Verma, J. (2006). In silico prediction of blood brain barrier permeability: an artificial neural network model. *J. Chem. Inf. Model.* 46, 289–297.

Giaume, C., Koulakoff, A., Roux, L., Holcman, D., and Rouach, N. (2010). Astroglial networks: a step further in neuroglial and gliovascular interactions. *Nat. Rev. Neurosci.* 11, 87–99.

Gold, M., and El Khoury, J. (2015). β -amyloid, microglia, and the inflammasome in Alzheimer's disease. In *Semin. Immunopathol* (Springer), pp. 607–611.

Grabert, K., Michoel, T., Karavolos, M.H., Clohisey, S., Baillie, J.K., Stevens, M.P., Freeman, T.C., Summers, K.M., and McColl, B.W. (2016). Microglial brain region- dependent diversity and selective regional sensitivities to aging. *Nat. Neurosci.* 19, 504.

Guo, J.L., and Lee, V.M. (2014). Cell-to-cell transmission of pathogenic proteins in neurodegenerative diseases. *Nat. Med.* 20, 130.

Halle, A., Hornung, V., Petzold, G.C., Stewart, C.R., Monks, B.G., Reinheckel, T., Fitzgerald, K.A., Latz, E., Moore, K.J., and Golenbock, D.T. (2008). The NALP3 inflammasome is involved in the innate immune response to amyloid- β . *Nat. Immunol.* 9, 857–865.

Harry, G.J. (2013). Microglia during development and aging. *Pharm. Ther.* 139, 313–326.

Hemmer, B., Kerschensteiner, M., and Korn, T. (2015). Role of the innate and adaptive immune responses in the course of multiple sclerosis. *Lancet Neurol.* 14, 406–419.

Heneka, M.T., Carson, M.J., El Khoury, J., Landreth, G.E., Brosseron, F., Feinstein, D.L., Jacobs, A.H., Wyss-Coray, T., Vitorica, J., Ransohoff, R.M., et al. (2015a). Neuroinflammation in Alzheimer's disease. *Lancet Neurol.* 14, 388–405.

Heneka, M.T., Golenbock, D.T., and Latz, E. (2015b). Innate immunity in Alzheimer's disease. *Nat. Immunol.* 16, 229.

Heneka, M.T., McManus, R.M., and Latz, E. (2018). Inflammasome signalling in brain function and neurodegenerative disease. *Nat. Rev. Neurosci.* 19, 610–621.

- Henstridge, C.M., Hyman, B.T., and Spire-Jones, T.L. (2019). Beyond the neuron–cellular interactions early in Alzheimer disease pathogenesis. *Nat. Rev. Neurosci.* *20*, 94–108.
- Heppner, F.L., Ransohoff, R.M., and Becher, B. (2015). Immune attack: the role of inflammation in Alzheimer's disease. *Nat. Rev. Neurosci.* *16*, 358–372.
- Hickman, S., Izzy, S., Sen, P., Morsett, L., and El Khoury, J. (2018). Microglia in neurodegeneration. *Nat. Neurosci.* *21*, 1359.
- Iturria-Medina, Y., Sotero, R.C., Toussaint, P.J., Evans, A.C., and Initiative, A.D.N. (2014). Epidemic spreading model to characterize misfolded proteins propagation in aging and associated neurodegenerative disorders. *PLoS Comput. Biol.* *10*, e1003956.
- Jiang, P., Gu, S., Pan, D., Fu, J., Sahu, A., Hu, X., Li, Z., Traugh, N., Bu, X., Li, B., et al. (2018). Signatures of T cell dysfunction and exclusion predict cancer immunotherapy response. *Nat. Med.* *24*, 1550–1558.
- Jirsa, V.K., Stacey, W.C., Quilichini, P.P., Ivanov, A.I., and Bernard, C. (2014). On the nature of seizure dynamics. *Brain* *137*, 2210–2230.
- Jucker, M., and Walker, L.C. (2018). Propagation and spread of pathogenic protein assemblies in neurodegenerative diseases. *Nat. Neurosci.* *21*, 1341.
- Karch, C.M., and Goate, A.M. (2015). Alzheimer's disease risk genes and mechanisms of disease pathogenesis. *Biol. Psychiatry* *77*, 43–51.
- Kettenmann, H., Hanisch, U.K., Noda, M., and Verkhratsky, A. (2011). Physiology of microglia. *Physiol. Rev.* *91*, 461–553.
- Khakh, B.S., and Sofroniew, M.V. (2015). Diversity of astrocyte functions and phenotypes in neural circuits. *Nat. Neurosci.* *18*, 942–952.
- Kolodkin, A., Simeonidis, E., Balling, R., and Westerhoff, H. (2012). Understanding complexity in neurodegenerative diseases: in silico reconstruction of emergence. *Front. Physiol.* *3*, 291.
- Korn, T., Magnus, T., and Jung, S. (2005). Autoantigen specific T cells inhibit glutamate uptake in astrocytes by decreasing expression of astrocytic glutamate transporter GLAST: a mechanism mediated by tumor necrosis factor- α . *FASEB J.* *19*, 1878–1880.
- Kreutzberg, G.W. (1996). Microglia: a sensor for pathological events in the CNS. *Trends Neurosci.* *19*, 312–318.
- Larochelle, C., Uphaus, T., Prat, A., and Zipp, F. (2016). Secondary progression in multiple sclerosis: neuronal exhaustion or distinct pathology? *Trends Neurosci.* *39*, 325–339.
- Lewis, N.E., Schramm, G., Bordbar, A., Schellenberger, J., Andersen, M.P., Cheng, J.K., Patel, N., Yee, A., Lewis, R.A., Eils, R., et al. (2010). Large-scale in silico modeling of metabolic interactions between cell types in the human brain. *Nat. Biotechnol.* *28*, 1279.
- Liblau, R.S., Gonzalez-Dunia, D., Wiendl, H., and Zipp, F. (2013). Neurons as targets for T cells in the nervous system. *Trends Neurosci.* *36*, 315–324.
- Liddel, S.A., Guttenplan, K.A., Clarke, L.E., Bennett, F.C., Bohlen, C.J., Schirmer, L., Bennett, M.L., Münch, A.E., Chung, W.S., Peterson, T.C., et al. (2017). Neurotoxic reactive astrocytes are induced by activated microglia. *Nature* *541*, 481–487.
- Lin, J.H.C., Lou, N., Kang, N., Takano, T., Hu, F., Han, X., Xu, Q., Lovatt, D., Torres, A., Willecke, K., et al. (2008). A central role of connexin 43 in hypoxic preconditioning. *J. Neurosci.* *28*, 681–695.
- Lin, J.H.C., Weigel, H., Cotrina, M.L., Liu, S., Bueno, E., Hansen, A.J., Hansen, T.W., Goldman, S., and Nedergaard, M. (1998). Gap-junction-mediated propagation and amplification of cell injury. *Nat. Neurosci.* *1*, 494–500.
- Lloret-Villas, A., Varusai, T., Juty, N., Laibe, C., Le Novere, N., Hermjakob, H., and Chelliah, V. (2017). The impact of mathematical modeling in understanding the mechanisms underlying neurodegeneration: evolving dimensions and future directions. *CPT: pharmacometrics Syst. Pharmacol.* *6*, 73–86.
- Lozano, D., Gonzales-Portillo, G.S., Acosta, S., de la Pena, I., Tajiri, N., Kaneko, Y., and Borlongan, C.V. (2015). Neuroinflammatory responses to traumatic brain injury: etiology, clinical consequences, and therapeutic opportunities. *Neuropsychiatr. Dis. Treat.* *11*, 97.
- Lublin, F.D., Reingold, S.C., Cohen, J.A., Cutter, G.R., Sørensen, P.S., Thompson, A.J., Wolinsky, J.S., Balcer, L.J., Banwell, B., Barkhof, F., et al. (2014). Defining the clinical course of multiple sclerosis. The 2013 revisions. *Neurology* *83*, 278–286.
- Luchtman, D., Gollan, R., Ellwardt, E., Birkenstock, J., Robohm, K., Siffrin, V., and Zipp, F. (2016). In vivo and in vitro effects of multiple sclerosis immunomodulatory therapeutics on glutamatergic excitotoxicity. *J. Neurochem.* *136*, 971–980.
- Mahad, D.H., Trapp, B.D., and Lassmann, H. (2015). Pathological mechanisms in progressive multiple sclerosis. *Lancet Neurol.* *14*, 183–193.
- Maragakis, N.J., and Rothstein, J.D. (2006). Mechanisms of disease: astrocytes in neurodegenerative disease. *Nat. Rev. Neurosci.* *9*, 679–689.
- Martins, I.F., Teixeira, A.L., Pinheiro, L., and Falcao, A.O. (2012). A bayesian approach to in silico blood-brain barrier penetration modeling. *J. Chem. Inf. Model.* *52*, 1686–1697.
- Mitosek-Szewczyk, K., Sulkowski, G., Stelmasiak, Z., and Strużyńska, L. (2008). Expression of glutamate transporters GLT-1 and GLAST in different regions of rat brain during the course of experimental autoimmune encephalomyelitis. *Neuroscience* *155*, 45–52.
- Nakase, T., Fushiki, S., and Naus, C.C. (2003). Astrocytic gap junctions composed of connexin 43 reduce apoptotic neuronal damage in cerebral ischemia. *Stroke* *34*, 1987–1993.
- Napoli, I., and Neumann, H. (2009). Microglial clearance function in health and disease. *Neuroscience* *158*, 1030–1038.
- Nativio, R., Donahue, G., Berson, A., Lan, Y., Amlie-Wolf, A., Tuzer, F., Toledo, J.B., Gosai, S.J., Gregory, B.D., Torres, C., et al. (2018). Dysregulation of the epigenetic landscape of normal aging in Alzheimer's disease. *Nat. Neurosci.* *21*, 497–505.
- Nave, K.A. (2010). Myelination and support of axonal integrity by glia. *Nature* *468*, 244–252.
- Nave, K.A., and Trapp, B.D. (2008). Axon-glia signaling and the glial support of axon function. *Annu. Rev. Neurosci.* *31*, 535–561.
- Neumann, H., Kotter, M.R., and Franklin, R.J.M. (2008). Debris clearance by microglia: an essential link between degeneration and regeneration. *Brain* *132*, 288–295.
- Nimmerjahn, A., Kirchhoff, F., and Helmchen, F. (2005). Resting microglial cells are highly dynamic surveillants of brain parenchyma in vivo. *Science* *308*, 1314–1318.
- Ofengeim, D., Ito, Y., Najafav, A., Zhang, Y., Shan, B., DeWitt, J.P., Ye, J., Zhang, X., Chang, A., Vakifahmetoglu-Norberg, H., et al. (2015). Activation of necroptosis in multiple sclerosis. *Cell Rep.* *10*, 1836–1849.
- Ouzounoglou, E., Kalamatanos, D., Emmanouilidou, E., Xilouri, M., Stefanis, L., Vekrellis, K., and Manolagos, E.S. (2014). In silico modeling of the effects of alpha-synuclein oligomerization on dopaminergic neuronal homeostasis. *BMC Syst. Biol.* *8*, 54.
- Parhizkar, S., Arzberger, T., Brendel, M., Kleinberger, G., Deussing, M., Focke, C., Nuscher, B., Xiong, M., Ghasemigharagoz, A., Katzmarski, N., et al. (2019). Loss of TREM2 function increases amyloid seeding but reduces plaque-associated apoE. *Nat. Neurosci.* *22*, 191–204.
- Petersen, M.A., and Dailey, M.E. (2004). Diverse microglial motility behaviors during clearance of dead cells in hippocampal slices. *Glia* *46*, 195–206.
- Petr, G.T., Sun, Y., Frederick, N.M., Zhou, Y., Dhamne, S.C., Hameed, M.Q., Miranda, C., Bedoya, E.A., Fischer, K.D., Armsen, W., et al. (2015). Conditional deletion of the glutamate transporter GLT-1 reveals that astrocytic GLT-1 protects against fatal epilepsy while neuronal GLT-1 contributes significantly to glutamate uptake into synaptosomes. *J. Neurosci.* *35*, 5187–5201.
- Pinheiro, M.A.L., Kooij, G., Mizze, M.R., Kamermans, A., Enzmann, G., Lyck, R., Schwaninger, M., Engelhardt, B., and de Vries, H.E. (2016). Immune cell trafficking across the barriers of the central nervous system in multiple sclerosis and stroke. *Biochim. Biophys. Acta* *1862*, 461–471.
- Poon, I.K.H., Lucas, C.D., Rossi, A.G., and Ravichandran, K.S. (2014). Apoptotic cell clearance: basic biology and therapeutic potential. *Nat. Rev. Immunol.* *14*, 166–180.

- Proctor, C.J., and Gray, D.A. (2010). Gsk3 and p53-is there a link in alzheimer's disease? *Mol. Neurodegener.* 5, 7.
- Proctor, C.J., and Lorimer, I.A. (2011). Modelling the role of the hsp70/hsp90 system in the maintenance of protein homeostasis. *PLoS One* 6, e22038.
- Ransohoff, R.M. (2016). A polarizing question: do M1 and M2 microglia exist? *Nat. Neurosci.* 19, 987–991.
- Rawji, K.S., Kappen, J., Tang, W., Teo, W., Plemel, J.R., Stys, P.K., and Yong, V.W. (2018). Deficient surveillance and phagocytic activity of myeloid cells within demyelinated lesions in ageing mice visualized by ex vivo live multiphoton imaging. *J. Neurosci.* 38, 1973–1988.
- Rohani, M., and Ghourchian, S. (2011). Fulminant multiple sclerosis (MS). *Neurol. Sci.* 32, 953–957.
- Santos, C.Y., Snyder, P.J., Wu, W.C., Zhang, M., Echeverria, A., and Alber, J. (2017). Pathophysiologic relationship between Alzheimer's disease, cerebrovascular disease, and cardiovascular risk: a review and synthesis. *Alzheimers Dement. (AMST)* 7, 69–87.
- Savill, J., and Fadok, V. (2000). Corpse clearance defines the meaning of cell death. *Nature* 407, 784–788.
- Schattling, B., Engler, J.B., Volkman, C., Rothammer, N., Woo, M.S., Petersen, M., Winkler, I., Kaufmann, M., Rosenkranz, S.C., Fejtova, A., et al. (2019). Bassoon proteinopathy drives neurodegeneration in multiple sclerosis. *Nat. Neurosci.* 22, 887–896.
- Sheedy, F.J., Grebe, A., Rayner, K.J., Kalantari, P., Ramkhalawon, B., Carpenter, S.B., Becker, C.E., Ediriweera, H.N., Mullick, A.E., Golenbock, D.T., et al. (2013). CD36 coordinates NLRP3 inflammasome activation by facilitating intracellular nucleation of soluble ligands into particulate ligands in sterile inflammation. *Nat. Immunol.* 14, 812–820.
- Shin, Y., and Brangwynne, C.P. (2017). Liquid phase condensation in cell physiology and disease. *Science* 357, eaaf4382.
- Siffrin, V., Radbruch, H., Glumm, R., Niesner, R., Paterka, M., Herz, J., Leuenberger, T., Lehmann, S.M., Luenstedt, S., Rinnenthal, J.L., et al. (2010). In vivo imaging of partially reversible Th17 cell-induced neuronal dysfunction in the course of encephalomyelitis. *Immunity* 33, 424–436.
- Sofroniew, M.V., and Vinters, H.V. (2010). Astrocytes: biology and pathology. *Acta Neuropathol.* 119, 7–35.
- Song, W.M., Joshita, S., Zhou, Y., Ulland, T.K., Gilfillan, S., and Colonna, M. (2018). Humanized TREM2 mice reveal microglia-intrinsic and -extrinsic effects of R47H polymorphism. *J. Exp. Med.* 215, 745–760.
- Spangenberg, E.E., Lee, R.J., Najafi, A.R., Rice, R.A., Elmore, M.R.P., Blurton-Jones, M., West, B.L., and Green, K.N. (2016). Eliminating microglia in Alzheimer's mice prevents neuronal loss without modulating amyloid- β pathology. *Brain* 139, 1265–1281.
- Stence, N., Waite, M., and Dailey, M.E. (2001). Dynamics of microglial activation: a confocal time-lapse analysis in hippocampal slices. *Glia* 33, 256–266.
- Surmeier, D.J., Obeso, J.A., and Halliday, G.M. (2017). Selective neuronal vulnerability in Parkinson disease. *Nat. Rev. Neurosci.* 18, 101–113.
- Tang, M.Y., Proctor, C.J., Woulfe, J., and Gray, D.A. (2010). Experimental and computational analysis of polyglutamine-mediated cytotoxicity. *PLoS Comput. Biol.* 6, e1000944, <https://doi.org/10.1371/journal.pcbi.1000944>.
- Tønnesen, J., Inavalli, V.K., and Nägerl, U.V. (2018). Super-resolution imaging of the extracellular space in living brain tissue. *Cell* 172, 1108–1121.
- Uemura, N., Uemura, M.T., Luk, K.C., Lee, V.M.Y., and Trojanowski, J.Q. (2020). Cell-to-cell transmission of tau and α -synuclein. *Trends Mol. Med.* 26, 936–952.
- Venegas, C., Kumar, S., Franklin, B.S., Dierkes, T., Brinkschulte, R., Tejera, D., Vieira-Saecker, A., Schwartz, S., Santarelli, F., Kummer, M.P., et al. (2017). Microglia-derived ASC specks cross-seed amyloid- β in Alzheimer's disease. *Nature* 552, 355–361.
- Vogel, J.W., Iturria-Medina, Y., Strandberg, O.T., Smith, R., Levitis, E., Evans, A.C., and Hansson, O. (2020). Spread of pathological tau proteins through communicating neurons in human alzheimer's disease. *Nat. Commun.* 11, 1–15.
- Von Bernhardi, R. (2007). Glial cell dysregulation: a new perspective on Alzheimer disease. *Neurotox Res.* 12, 215–232.
- Von Bernhardi, R., Eugenin-von Bernhardi, L., and Eugenin, J. (2015). Microglial cell dysregulation in brain aging and neurodegeneration. *Front. Aging Neurosci.* 7, 124.
- Weickenmeier, J., Kuhl, E., and Goriely, A. (2018). Multiphysics of prionlike diseases: progression and atrophy. *Phys. Rev. Lett.* 121, 158101.
- Witting, A., Müller, P., Herrmann, A., Kettenmann, H., and Nolte, C. (2000). Phagocytic clearance of apoptotic neurons by microglia/brain macrophages in vitro. *J. Neurochem.* 75, 1060–1070.
- Wolf, Y., Yona, S., Kim, K.W., and Jung, S. (2013). Microglia, seen from the CX3CR1 angle. *Front. Cell. Neurosci.* 7, 26.
- Yuan, J., Amin, P., and Ofengeim, D. (2018). Necroptosis and RIPK1-mediated neuroinflammation in CNS diseases. *Nat. Rev. Neurosci.* 20, 19–33.
- Yuraszck, T.M., Neveu, P., Rodriguez-Fernandez, M., Robinson, A., Kosik, K.S., and Doyle, F.J., III (2010). Vulnerabilities in the tau network and the role of ultrasensitive points in tau pathophysiology. *PLoS Comput. Biol.* 6, e1000997, <https://doi.org/10.1371/journal.pcbi.1000997>.
- Zamanian, J.L., Xu, L., Foo, L.C., Nouri, N., Zhou, L., Giffard, R.G., and Barres, B.A. (2012). Genomic analysis of reactive astrogliosis. *J. Neurosci.* 32, 6391–6410.
- Zhang, H., and Xiao, P. (2018). Seizure dynamics of coupled oscillators with epileptor field model. *Int. J. Bifurcation Chaos* 28, 1850041.
- Zott, B., Simon, M.M., Hong, W., Unger, F., Chen-Engerer, H.J., Frosch, M.P., Sakmann, B., Walsh, D.M., and Konnerth, A. (2019). A vicious cycle of β amyloid-dependent neuronal hyperactivation. *Science* 365, 559–565.

iScience, Volume 23

Supplemental Information

How Repair-or-Dispose Decisions

Under Stress Can Initiate Disease Progression

Andreas Nold, Danylo Batulin, Katharina Birkner, Stefan Bittner, and Tatjana Tchumatchenko

Supplemental Information

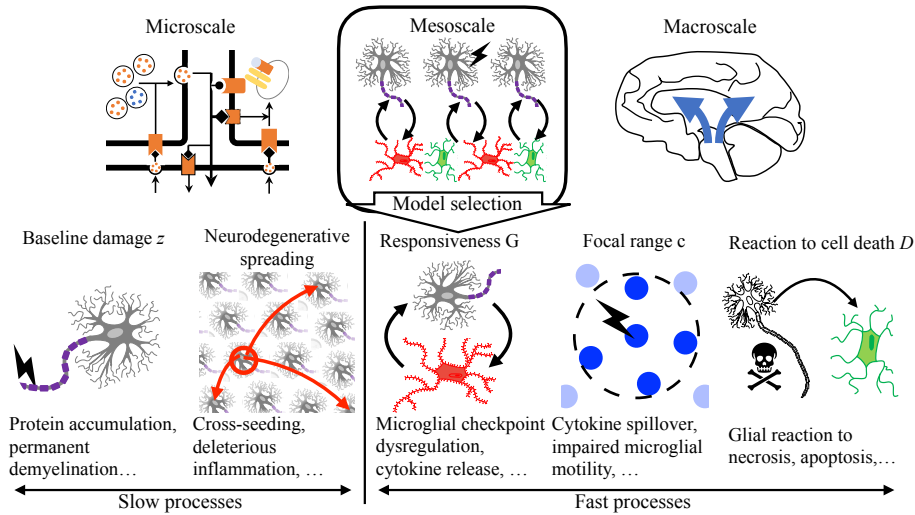


Figure S1: **Five classes of neuron-glia crosstalk are included in a mesoscale model. Related to Figure 2.** We choose a mesoscopic modeling level which generalizes tissue response to a small number of observable factors. It mediates between the microscopic level of cellular and molecular processes (Jolivet et al., 2015) (top left) and the macroscopic level of interacting brain regions (Jucker and Walker, 2013; Weickenmeier et al., 2018) (top right). The model includes the following distinct properties of glia-neuron crosstalk: (i) accumulation of non-repairable baseline damage (z); (ii) slow neuron-to-neuron spreading of baseline damage (S); (iii) glial responsiveness to neuronal damage (G); (iv) focal range of glial reactivity (c); (v) tissue reaction to cell death (D).

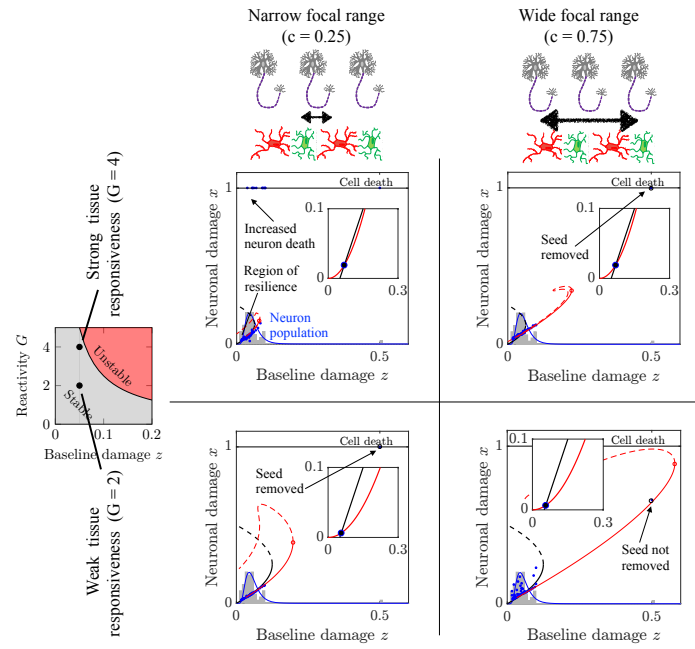


Figure S2: **Functional tissue resilience requires tuning between focal range c and tissue responsiveness G .** Related to **Figure 3**. Black solid and dashed lines represent stable and unstable steady states in the mean field limit. Red solid and dashed lines represent stable and unstable steady states of one cell for a given (z_n) -distribution. Blue dots represent a population of 200 cells, taken from a log-normal distribution (blue lines). Grey bars represent the histogram of their (z_n) -distribution. Note that some cells are dead (death threshold at unity). For a narrow focal range ($c = 0.25$), cells react more independent of each other (see left column). For a wide focal range ($c = 0.75$), population effects allow for regional compensation of locally elevated stress levels (see top right), but also of rescue of seeds, if the responsiveness G is attenuated (see bottom right). Red and black lines of the insets show mean field damage inducing and damage reducing effects Gx^2 and $x - z$, respectively, as a function of acute damage x .

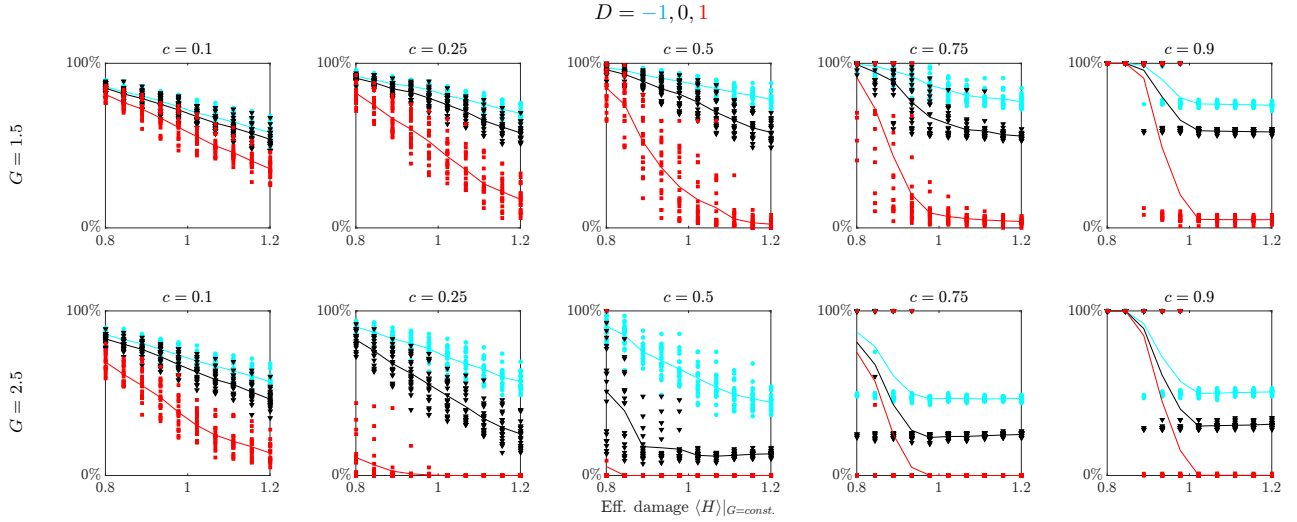
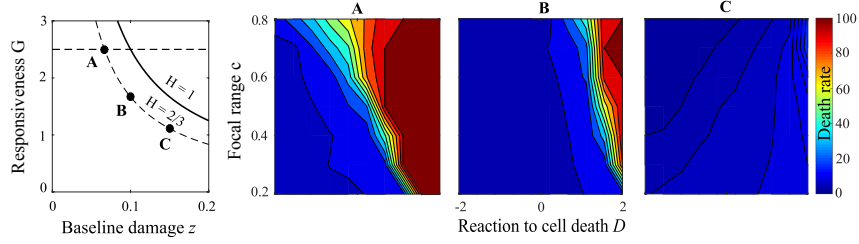
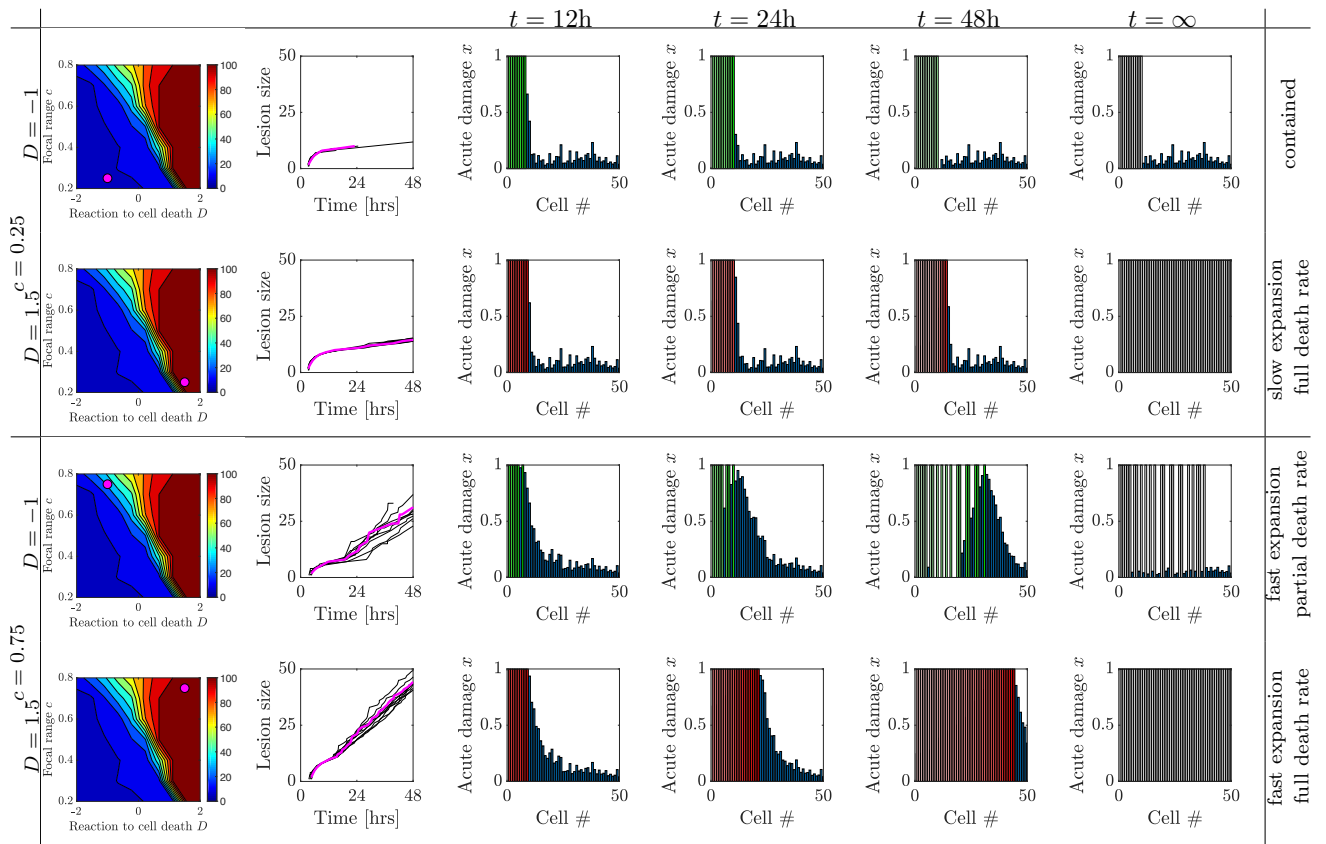


Figure S3: **Critical transition after population increase of baseline damage. Related to Figure 6.** Survival rates after spontaneous cell death for different strengths of responsiveness G for different levels of focal range c , plotted as a function of the effective damage parameter $\langle H \rangle|_{G=const.} = \langle 4Gz \rangle|_{G=const.}$. Simulations with anti-inflammatory, neutral or pro-inflammatory reaction to cell death ($D = -1, 0, 1$) are represented by cyan, black and red lines, respectively. Each symbol represents one distribution of baseline damage levels (z_n), and solid lines connect mean values. Parameters: $N = 100$ in a periodic one-dimensional domain, $t_{\max} = 10$ days, 20 runs per parameter set. Systems with a wide focal range ($c \rightarrow 1$) exhibit step-like transitions, for which all cells survive until the critical point is reached, beyond which a steep decrease in survival rates is seen. In contrast, for narrow focal ranges ($c \rightarrow 0$), the tissue reacts separately to the stress levels of individual cells, therefore allowing for a gradual decline of survival rates. Protective tissue reactions to cell death ($D = -1$) can act as a barrier for the spread of damage and stabilize cell loss after crossing the critical transition. If protective effects to cell death are attenuated ($D = 0$) or become toxic ($D = 1$), then the death of the first cell sets off a domino-like knock-on effect that can lead to the early death of large parts of the cell assembly. Tissue with intermediate focal range (e.g. $c = 0.5$) is particularly vulnerable to this effect, because local stress by a dying cell fully acts on the neighboring cell, and is not distributed across the tissue. This means that even though the system is stable locally, i.e. small perturbations to the damage levels can be compensated for, it is not stable with respect to the impact of one dying cell, which sets off a propagating lesion.



(a) Death rate of a subthreshold stable tissue following an external attack for different baseline damage levels z , as a function of tissue reaction to cell death D and focal range c , for effective responsiveness $\langle H \rangle = 4G(z) = 2/3$.



(b) Snapshots of an expanding lesion, initiated by an external injury as in panel **A** of (a) ($G = 2.5$, $\langle H \rangle = 2/3$), for different levels of focal range c and tissue reaction to cell death D . Magenta circles in the plots of the first column depict the chosen parameter set. The colorscale in the first column represents the death rate, as in (a). The second column depicts lesion front paths for 10 (z_n)-distributions. The snapshot panels ($t = 12\text{h}, 24\text{h}, \dots$) show acute damage values x_n for the path represented by the magenta line. Each bar represents one cell. Blue bars represent amount of damage of alive cells. Bars that reach unity are dead cells. Levels of red and green represents the level of damage-inducing and protective tissue reaction to cell death, respectively.

Figure S4: **Analysis of primed tissue. Related to Figure 6** Impact of an acute attack on a stable tissue with 100 cells. Here, the stressor function $f_{\text{ext},n} = e^{-t/\tau_{\text{ext}}} [1 - \frac{n}{N_{\text{ext}}}]_+$, is added to the right-hand side of Eq. 3 $\tau_{\text{ext}} = 48\text{ h}$ and $N_{\text{ext}} = 10$. Acute attacks can initiate wave-like expanding lesions for highly reactive tissues. For a narrow focal range ($c = 0.25$), damage spreads in a domino-like manner from cell to cell. It is contained if tissue reaction to cell-death is protective ($D = -1$), but spreads slowly if tissue reaction to cell death is damage-inducing ($D = 1$). For a wide focal range ($c = 0.75$), a large enough part of the cell population needs to be sufficiently damaged to activate the toxic feedback loop. In this case, the lesion spreads quickly, leading to partial and complete cell death for protective and inflammatory tissue reactions D , respectively.

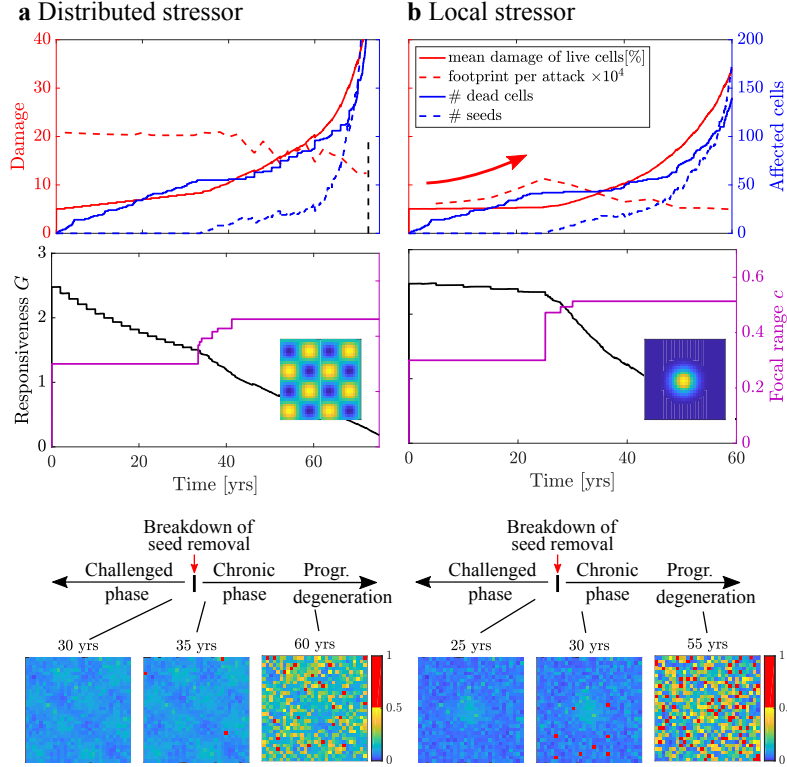


Figure S5: **Long-term stress exposure. Related to Figure 8** **Left:** Frequent, weak distributed stressor across the tissue. Gradual adaptation of reactivity G to higher mean damage levels leads to a breakdown of seed removal. **Right:** Repeated, stronger stressor at the center of the domain. Repeated local attacks require an adaptation of the focal range c to maintain short-term stability, leading to a breakdown of seed removal. Prior to this breakdown, the footprint of each perturbation increases (see red arrows). In both scenarios, after the breakdown of seed removal, cell death is first offset because seeds are maintained in the tissue which leads to increasing damage levels. Eventually, cell death rates increase too. Bottom: Baseline damage levels z prior to, immediately after, and long after breakdown of seed removal. Seeds are shown in red. The insets of the graphs of the second row depict the imposed stress pattern. Here, $\tau_\infty = 50$ yrs. For model computations without adaptation of G and c , see Figure S6. The following randomly induced stressors were induced: (A) Seeds are induced independently with frequency $\nu = 1/(10\tau_\infty)$. (B) Subthreshold stressors $f_{ext,n}(t) = s(\mathbf{r}_n) \sum_k h(t - t_k)$ are added to the acute cell state are induced at times t_k at rate $1/(2\text{yrs})$ and $1/(5\text{yrs})$. Localized subthreshold stressors are modeled with $s(\mathbf{r}_n) = e^{-|\mathbf{r}_n - \mathbf{r}_c|^2/(2\sigma^2)}$ and $\mathbf{r}_c = (n/2, n/2)$. Distributed subthreshold stressors in Figure S5a are modeled with $s(\mathbf{r}_n) = (1 + \sin(4\pi(\mathbf{r}_n)_1/n) \sin(4\pi(\mathbf{r}_n)_2/n))/2$. The temporal evolution is $h(t) = \bar{A}\Theta(t)(1 + \tanh((12h - t)/4h))/2$ with heaviside function $\Theta(t)$ and $\bar{A} = 0.1$. After equilibration after each subthreshold stressor at times t_k , baseline damage is increased by $\Delta z = A \int_{t_k}^\infty (x_n - x_n^{eq}) dt$, where x_n^{eq} is the equilibrium state before induction of the subthreshold stressor. $A = 1/500$ and $1/200$ for distributed and local stressors, respectively. After each subthreshold stressor, the parameters c and G were adapted such that: $4G(z) < H = 0.5$. The focal range was adapted such that the maximal eigenvalue λ of Eq. 2 remains $\lambda < -0.1/\tau$.

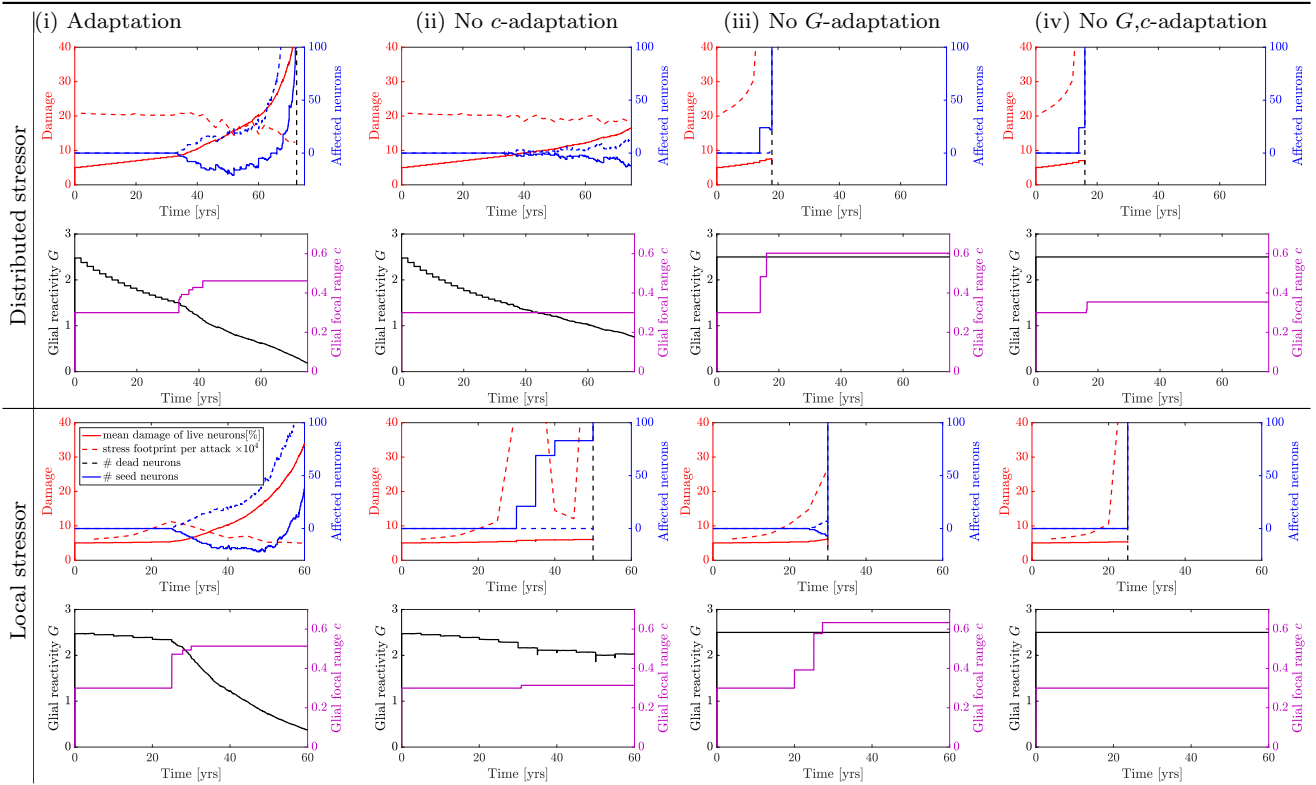


Figure S6: **Lack of adaptation leads to early catastrophic cell loss.** Related to [Figure 8](#) Effect of adaptation of responsiveness G and focal range c for distributed and local stressors as in [Figure S5](#). The first column depicts the results as in [Figure S5](#) of the main manuscript. In the subsequent columns, we deactivate adaptation of c (ii), adaptation of G (iii), and both G and c (iv). In all cases, c is not allowed to adapt beyond 0.6. The black dashed line represents the time point of catastrophic cell loss of more than 100 cells (11%). It is seen how no adaptation leads to early catastrophic cell loss. The distributed stressor model is stabilized by G -adaptation, and the local stressor model is stabilized by both G and c adaptation.

Transparent Methods

S1. Details of numerical simulations

If not stated otherwise, baseline neuronal damage levels z_n are independently drawn from a log-normal distribution, where mean and standard deviation are given in the figure captions. The spatial coupling term $s(r)$ in Eq. 3 is normalized such that in the given domain, $\sum_m s(|\mathbf{r}_n - \mathbf{r}_m|) = 1$. Simulations at the fast time scale were computed with step $\Delta t = 0.005$ hrs, with a first-order Euler forward method. Simulations were implemented on Matlab2018a.

S2. Mean field and steady state solutions

The mean field limit of Eq. 3 is defined by $x_n = x, g_n = g, z_n = z$ constant for all n . In this case, if the cells are alive ($x < 1$), then $g = Gx^2$, and the acute damage x solves $\tau \frac{dx}{dt} = -(x - z) + Gx^2$, with steady states given by $x_{\pm} = (1 \pm \sqrt{1 - 4Gz})/(2G)$ if $z < z_{\text{crit}} = 1/(4G)$. Here, x_+ and x_- are the unstable and stable solutions, depicted in Figure 3. The critical point, beyond which no stationary solution exists, is given by z_{crit} , see also Figure S2.

S3. Focal range c

The interplay between responsiveness G and focal range c determines the tissue reaction to cell damage. It therefore determines whether seed removal is functional or not. In Figure S2 the population effect of four configurations of G and c is shown as an example. In the following, we study the behavior of Eq. 3 of the main manuscript in the limit of very narrow and very wide focal ranges.

If the focal range is very narrow, $c \rightarrow 0$, then $\sum_m s(|\mathbf{r}_n - \mathbf{r}_m|)g_m \rightarrow g_n$, and we obtain independent ordinary differential equations for all n :

$$\tau \frac{dx_n}{dt} = -(x_n - z_n) + g_n. \quad (\text{S1})$$

The results of the mean field section then hold individually for each cell. One side-effect of an increased focal range is that single cells can be maintained, even though their baseline damage z_n exceeds the critical value z_{crit} (see Figures 5 and S2).

If the focal range is very wide, $c \rightarrow 1$, we map the discrete values of n onto the spatial variable $\eta = \Delta \cdot n$ with $\Delta = -\log c$. As $c \rightarrow 1$, Δ decreases to zero, allowing us to define state variables as functions of η : $x(\eta), g(\eta), z(\eta)$. In the one-dimensional case, d_n in Eq. 3 becomes

$$\begin{aligned} \frac{1-c}{1+c} \sum_{m=-\infty}^{\infty} c^{|n-m|} g_m &= \frac{1-c}{1+c} \sum_{m=-\infty}^{\infty} e^{-\Delta|n-m|} g_m \\ &\xrightarrow{c \rightarrow 1} \frac{\Delta}{2} \sum_{m=-\infty}^{\infty} e^{-\Delta|n-m|} g_m \\ &\xrightarrow{\Delta \rightarrow 0} \frac{1}{2} \int_{-\infty}^{\infty} e^{-|\eta-\eta'|} g(\eta') d\eta', \end{aligned}$$

where we used that $\frac{1-c}{1+c} \rightarrow \frac{\Delta}{2} + O(c-1)^3$ as $c \rightarrow 1$. Eq. 3 then becomes an integral equation

$$\tau \frac{\partial x}{\partial t} = -(x - z) + \frac{1}{2} \int_{-\infty}^{\infty} e^{-|\eta-\eta'|} g(\eta') d\eta'. \quad (\text{S2})$$

Therefore, for highly imprecise reactivities the characteristic length scale is Δ and the influence of one cell on another decays exponentially on that length scale. This can be observed in the snapshots of Figure [S4](#)

Critical transitions. High levels of baseline damage z can destabilize the tissue. This can happen in two ways: First, a sudden large increase of $\langle z \rangle$ can lead to spontaneous cell death across the tissue (see Figure [S3](#)). This has different consequences, depending on the focal range c : Systems with narrow focal ranges allow for gradual cell loss when z increases, but systems with wide focal range c react suddenly and collectively. This population effect has been observed in many other biological and ecological systems, for instance when coral reefs are repaired by ‘mobile link organisms’ from nearby reefs ([Scheffer et al. 2012](#)).

As discussed in the main manuscript, in addition to this classical transition, our model also reveals a metastable ‘primed state’ for intermediate levels of z (see Figure [6](#)). Under normal conditions, this primed tissue appears to be healthy. However, in the event of strong enough perturbation, the tissue amplifies damage and may initiate a wave-like spreading lesion. In general, anti-inflammatory reactions to cell death (negative D) protect the surrounding tissue against these knock-on effects. If this protection, however, is attenuated, and focal range is wide, then acute attacks can cause widespread damage. Wide focal ranges (high c) and pro-inflammatory reaction to cell death (high D) increases damage. Importantly in this case, the risk of acute short-term damage amplification is more pronounced for a system with intact, high, responsiveness G (see Figure [S4](#) for details).

S4. Seeding parameter S

Equation [1](#) describes slow damage propagation. We can add a term that represents seeding events that happen at rate ν . After non-dimensionalization, we obtain

$$\frac{dz_n}{dt'} = \frac{1}{\nu\tau_\infty} \sum_{m \in \mathcal{C}_n} [z_m - \theta]_+ + z_{\text{cliff}} \sum_k \delta(t' - t'_{k,n}), \quad (\text{S3})$$

with dimensionless timescale $t' = t\nu$, and where the seeding events $t'_{k,n}$ take place at a rate of one (with respect to the new timescale t'). The early, linear damage propagation is then described by the dimensionless parameter

$$S = \frac{M}{\nu\tau_\infty}. \quad (\text{S4})$$

S represents the balance of the spreading strength M , given by the number of elements in \mathcal{C}_n and speed $1/\tau_\infty$, to the rate of independent self-induced seeding events ν .

Supplemental References

Jolivet, R., Coggan, J.S., Allaman, I., Magistretti, P.J., 2015. Multi-timescale modeling of activity-dependent metabolic coupling in the neuron-glia-vasculature ensemble. *PLoS Comput Biol* 11, e1004036.

Jucker, M., Walker, L.C., 2013. Self-propagation of pathogenic protein aggregates in neurodegenerative diseases. *Nature* 501, 45.

Scheffer, M., Carpenter, S.R., Lenton, T.M., Bascompte, J., Brock, W., Dakos, V., van de Koppel, J., van de Leemput, I.A., Levin, S.A., van Nes, E.H., et al., 2012. Anticipating critical transitions. *Science* 338, 344–348.